FACULDADE DE ENGENHARIA DA UNIVERSIDADE DO PORTO

A Thermal Energy Balance Model for a Wood Industry in Oliveira do Hospital

Ricardo Pereira da Costa de Jesus Rosa

Master Degree in Mechanical Engineering

Supervisor: Prof. Eliseu Monteiro

Second Supervisor: Eng.º Abílio Guimarães

June 21, 2024

A Thermal Energy Balance Model for a Wood Industry in Oliveira do Hospital

Ricardo Pereira da Costa de Jesus Rosa

Master Degree in Mechanical Engineering

June 21, 2024

ABSTRACT

The rise in energy sources costs has a significant impact on industries. Continuous improvement of energy management plays a role in production costs and ultimately in a company's competitiveness. Sonae Arauco wood-based products industrial plant in Oliveira do Hospital, supported by its biomass thermal energy plant, is an intensive consumer of thermal energy.

This research aims to develop a model to identify, map and quantify the plant's thermal energy production and consumption. This project includes a review of biomass usage, boilers and the types of thermal energy consumers in the plant namely dryers and hot presses, followed by on-site empirical investigations. Data collection and measurements at key energy flow points enabled the creation of the thermal energy balance model with calculated results for 2023 operation.

The thermal energy balance model revealed that in 2023, biomass was the primary energy source for the plant, with an average biomass flow of 4.45 t/h. Biomass accounted for a total of 183 551 MWh, representing 61 % (*toe*) of the total energy consumption in that year. The wood particle dryers were the main thermal energy consumers, with BSH using a total of 34 919 MWh and Recalor using 28 580 MWh. Consumption patterns and correlations between energy use and production variables were founded, underscoring the importance of thermal energy management integration with production processes.

Ensuring that the required thermal energy control points are covered with measurement instruments enhances the accuracy and reliability of the developed model results. Therefore, the installation of instrumentation at identified control points has been proposed.

Keywords: thermal energy, energy management, biomass.

RESUMO

Modelo de Balanço Energético Térmico para uma Indústria de Madeira em Oliveira do Hospital

O aumento dos custos das fontes de energia tem um impacto significativo nas indústrias. A melhoria contínua da gestão de energia reflete-se nos custos de produção e, consequentemente, na competitividade de uma empresa. A unidade industrial de produtos derivados de madeira da Sonae Arauco em Oliveira do Hospital, apoiada pela sua central de energia térmica a biomassa, é uma consumidora intensiva de energia térmica.

Esta investigação procura desenvolver um modelo adequado para identificar, mapear e quantificar a produção e consumo de energia térmica da fábrica. Este projeto inclui uma análise teórica da utilização de biomassa, caldeiras e dos tipos de consumidores de energia térmica presentes na fábrica, nomeadamente secadores e prensas a quente, seguido por investigações empíricas no local. A recolha de dados e medições nos principais pontos do fluxo energético permitiram a criação de um modelo de balanço de energia térmica com resultados calculados para a operação de 2023.

Os resultados do modelo desenvolvido aplicado a 2023 revelaram que a biomassa, com um caudal médio de 4,45 t/h, foi a principal fonte de energia da fábrica. A biomassa contabilizou um total de 183551 MWh, representando 61% (tep) do consumo energético total desse ano. Os secador de partículas de madeira foram os maiores consumidores de energia térmica, com o BSH a consumir 34919 MWh e o Recalor a consumir 28580 MWh. Foram estabelecidos padrões de consumo e correlações entre o uso de energia e as variáveis de produção, realçando a importância da integração da gestão de energia térmica com os processos produtivos.

Assegurar que os parâmetros necessários para controlo do fluxo de energia térmica são cobertos por instrumentos de medição garante uma maior precisão e fiabilidade dos resultados do modelo desenvolvido. Assim, foi proposta a instalação de instrumentação em pontos de controlo identificados.

Palavras-chave: energia térmica, gestão de energia, biomassa.

AGRADECIMENTOS

Quero expressar o meu sincero agradecimento a quem marcou o meu percuso. O meu reconhecimento especial:

Ao Professor Eliseu Monteiro, da Faculdade de Engenharia da Universidade do Porto, por ter aceitado orientar este trabalho e por ter contribuído com disponibilidade, exigência e rigor ciêntifico.

Ao Engenheiro Abílio Guimarães, Gestor de Energia corporativo da Sonae Arauco e meu coorientador, pela oportunidade, voto de confiança, ensinamentos e companheirismo que muito contribuiu para a realização deste trabalho.

Ao Engenheiro José Bernardo Lobo, Diretor de Manutenção da Sonae Arauco em Oliveira do Hospital e restante equipa de manutenção, João Pedro Batista, António Borges, Rafael Pires, Bruno Poceiro, Luís Marques e Fernando Duarte por me terem acolhido abertamente na fábrica, pela partilha de conhecimentos e experiências, sempre pautada por profissionalismo e boa disposição e que muito contribuiram para tornarem este trabalho numa experiência tão gratificante.

À minha família e amigos, dos quais guardo momentos fantásticos.

Aos meus pais, por serem o meu exemplo e permitirem que tudo isto seja possível. Deram-me valores e ferramentas para alcancar os meus sonhos. Por estarem sempre presentes em cada desafio e em cada vitória. Obrigado.

Ricardo Rosa

TABLE OF CONTENTS

LIST OF FIGURES

LIST OF TABLES

ABBREVIATIONS AND SYMBOLS

List of abbreviations

EES	Engineering Equation Solver
ESV	Electronic Speed Variator
MDF	Medium-density Fiberboard
MFC	Melamine Facing Chipboard
OH	Oliveira do Hospital
PB	Particle Board
PID	Proportional Integral Derivative

List of symbols

C_p	Constant pressure specific heat	[J/(kg·K)]
D_h	Hydraulic diameter	[mm]
db	Dry basis	
FC	Fixed carbon content	
HHV	Higher heating value	[MJ/kg]
LHV	Lower heating value	[MJ/kg]
$\dot{m}$	Mass flow rate	[kg/s]
Q	Thermal energy	[J]
$\dot{Q}$	Thermal power	[W]
T	Temperature	[°C]
$\dot{V}$	Volumetric flow rate	[m^3/h]
W	Moisture content	[%]
wb	Wet basis	
$wt.\%$	Weight fraction	[%]
η_{boiler}	Boiler efficiency	[%]
λ	Latent heat of vaporization	[kJ/kg]
ρ	Density	[kg/m^3]

List of subscripts

clp	Relative to continuous line press
dry	Relative to drying wood particles
$evap$	Relative to water evaporation
f	Relative to final state
i	Relative to initial state
to	Relative to thermal oil
un	Relative to lower heating circuit
up	Relative to upper heating circuit
w	Relative to water
w_i	Relative to initial state of wood particles

Chapter 1

INTRODUCTION

Energy is the main factor underlying human growth and civilization. Through time, the need to develop and research new approaches and strategies to use energy effectively without endangering social, economic, or environmental issues has risen.

The industrial sectors have concerns about a potential shortage of energy in the future due to factors such as the use of non-renewable resources for energy transformation, the inevitable depletion of fossil fuels, the wide fluctuations in oil prices on global markets, and environmental pollution from the greenhouse effect-causing emissions of CO_2 and CO. These elements have aided in the hunt for new energy transformation technologies. Portugal holds a significant potential for the use of renewable energies. This potential stems from the territory's features, location, and abundance of natural resources, notably hydro, wind, biomass, and solar.

Therefore, research of methods and strategies for improving systems and processes' energy efficiency is necessary. Thermodynamics is essential in systems and processes that involve the transportation and transformation of energy. Its laws make it possible to calculate the efficiency and potential losses.

This study presents a mapping of a thermal energy process using biomass and a tool for improving its efficiency, reducing energy losses and, consequently, greenhouse gas emissions, promoting the sustainability of energy production and consumption.

1.1 Project framework and motivation

This dissertation carried out as part of the Master's degree in Mechanical Engineering at the Faculty of Engineering of the University of Porto, was developed in an internship environment at the Sonae Arauco plant in Oliveira do Hospital.

The search for energy efficiency is a constant concern for the industrial plant under analysis, especially during fluctuations in energy prices.

In these factories where the main raw material is wood, to produce wood-based products, efficiency in the production of thermal energy using wood itself was often overlooked. This was precisely due to its easy availability and relatively low cost.

However, this tendency to neglect is being reconsidered in light of the growing imperatives of sustainability and energy efficiency as well as the rising price of biomass. In this context, it was recognized the need to evaluate and optimize the thermal energy production and consumption at the industrial plants, considering that a small improvement of a boiler and thermal energy transfer efficiency can lead to significant energy savings, a reduction in polluting

gas emissions (Barma et al., 2017), along with a positive impact in the operational results of the company.

1.2 Sonae Arauco

Sonae Arauco resulted in a partnership signed in 2016 between Sonae Indústria and Arauco. Today, it is one of the largest wood-based solutions companies in the world, with 20 industrial and commercial units in 9 countries. It has a production capacity of around 3.920 million m^3 and a turnover of 950 million euros.

Sonae Indústria was founded in 1959 in Maia as Sociedade Nacional de Estratificados, dedicated to the production of wood-based panels, a material that was beginning to be used in the construction, furniture, and decoration sectors.

Arauco is one of the largest producers and managers of renewable forest resources. It was founded in Chile in 1970 to improve and increase its dominance in the forest through research and sustainable practices.

1.3 Project aims and objectives

This project aims to create an energy balance model that can identify the flow of combustible materials used in the production of thermal energy, as well as the main consumers at the Oliveira do Hospital plant. With the energy balance model established it will be identified opportunities for energy optimization, which may help to reduce consumption and promote energy efficiency.

1.4 Research methodology

In this work, it was first investigated the utilization of biomass, boilers, dryers and presses within the context of industrial operations. With the comprehension of these concepts, it was conducted an empirical investigation at the plant site.

1.5 Structure

This dissertation report is divided into six chapters. The first introduction chapter provides an overview of the project, introduces the company and the plant where the research was conducted and details the methodology employed in the study. Chapter 2 conducts a literature review with a comprehensive study of biomass utilization, boilers technology, drying and pressing equipment, which are concepts relevant to establish a theoretical foundation for the study. The third chapter provides a detailed description of the problem, including the plant infrastructure, thermal energy plant and thermal energy users equipment and operational processes and also outlines how the thermal energy balance model will be constructed and implemented. Then, the thermal energy balance model with the collected data is presented in Chapter 4. The final

part of the report presents a comprehensive analysis of the results obtained from the suggested model with proposed potential improvements. This report ends with a summary of the key findings and conclusions drawn from the study while offering directions for further investigation into the studied plant.

Chapter 2

LITERATURE REVIEW

2.1 Biomass

Biomass refers to organic matter, both living and dead, including plants, animals, and their waste. It also includes waste products resulting from the conversion of materials from animal and plant sources, such as those from the paper and cellulose industry, the food industry, and organic waste from commerce or industry in general (de Pinho, 2016).

Biomass used at Sonae Arauco's thermal energy plant in Oliveira do Hospital is bought mainly in the form of recycled chips and bark. Moreover, dust residues from the process are also used.

(a) Recycled chips.

(b) Bark.

(c) Dust residues.

Figure 2.1 – Types of biomass used at Oliveira do Hospital thermal energy plant.

2.1.1 Forest residues

Forest residues are a source of biomass with significant potential, with studies indicating that they can make a significant contribution to meeting the world's energy needs (Mateos, 2019).

The use of forest residues as fuel is a solution to waste management problems and can also prevent the risk of forest fires. However, there are also potential disadvantages to its use, such as the impact on biodiversity and managing the sustainability of deforestation, which is an aggravated risk in developing countries (Gregg and Smith, 2010).

Portugal holds a significant potential to use forest residues as biomass, with a third of land area being forest primarily covered with *Pinus Pinaster* (49 690 kt) and *Eucalyptus* (36 252 kt), which can result in an installed power of 264 MW (Monteiro et al., 2012).

2.1.2 Industrial residues

Industrial waste, including waste from medium-density fiberboard (MDF), particleboard (PB), and other wood-based furniture industries, has significant potential for use as biomass. These residues can be used to produce pellets or burned directly, offering advantages such as turning industrial waste into a renewable energy source and producing less emissions and ash when compared with agricultural residues. However, their use presents inherent challenges, including economic factors, as these residues may require treatment and processing before burning (Monteiro et al., 2012).

2.1.3 Biomass advantages

Biomass is a renewable source of energy since it will always be possible to grow crops and waste will always be produced, with a very short renewal time, unlike fossil fuels (de Pinho, 2016).

Plant biomass is organic matter resulting from the process of photosynthesis. Thus, the energy contained in biomass comes from the sun. In the process of photosynthesis, the plant converts, together with carbon dioxide, energy in the form of solar radiation into chemical energy in the form of glucose, as depicted in equation 2.1 (Saidur et al., 2011).

$$6H_2O + 6CO_2 + Radiant\ energy \longrightarrow C_6H_{12}O_6 + 6O_2 \tag{2.1}$$

When biomass is combusted, carbon dioxide is formed and released into the atmosphere as a result of the reaction between carbon and oxygen. However, the amount of carbon dioxide released is equal to the amount that was captured during the process of photosynthesis (Saidur et al., 2011). Therefore, using biomass as fuel is considered a carbon-neutral process, known as the carbon cycle (Figure 2.2).

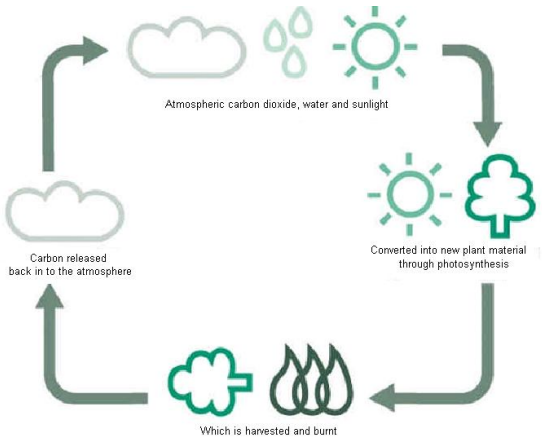

Figure 2.2 – Carbon cycle in biomass production and consumption (of Strathclyde, 2008).

2.1.4 Biomass consumption

Globally, more than 3 billion people depend on biomass, such as wood, charcoal, agricultural and forestry waste, animal excrement, and mineral coal, as their primary domestic energy sources (de Pinho, 2016). In 2019, biomass accounted for 12% of the world's energy consumption (Figure 2.3).

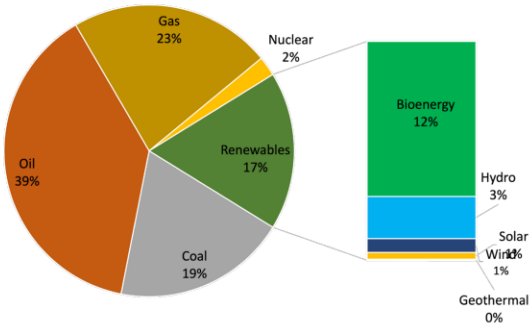

Figure 2.3 – Gross final energy consumption in 2019 (WBA, 2022).

2.1.5 Biomass properties

To properly use biomass as fuel, certain physical and chemical properties must be considered, namely moisture content, wet and dry weight, ash content, density, chemical composition and energy content. These properties will later constrain the design and operation of biomass boilers.

When the composition of wood is considered the amount of moisture contained, the information in question is said to be given on a wet basis (wb), whereas if the basis is dry matter, it is referred to on a dry basis (db) (de Pinho, 2016).

These physical properties vary significantly, and those variations can affect the process. The moisture content can vary from a few wt% moisture to over 70 wt% depending on the origin of the biomass, ambient conditions, time of year, and storage conditions. The higher

the moisture content the lower the storage durability and combustion performance (ORANG and TRAN, 2015), with the limit of 60 % moisture content from which the combustion can no longer be maintained (van Loo and Koppejan, 2008).

Ash, as an inert matter, does not contribute to heat during combustion. Moreover, its presence can have substantial effects on the efficiency, the integrity of a boiler and emissions. Ash can deposit along critical components, such as heat exchangers, impacting heat transfer and leading to corrosion (Skrifvars et al., 2004).

To analyze the properties of biomass, one can conduct a proximate or an ultimate analysis.

The proximate analysis reveals the composition of biomass in terms of moisture content, volatile matter, fixed carbon, and ash. It is a relatively simple and inexpensive process. Table 2.1 shows the values obtained from proximate analysis for some types of fuel.

Table 2.1 – Comparison of proximate analysis of some biomass types (Klass, 1998)

Fuel	Fixed carbon [wt % db]	Volatile Matter [wt% db]	Ash [wt% db]
Ponderosa pine	12.8	87.0	0.2
Eucalyptus globulus	17.3	81.6	1.1
Cedar	21.0	77.0	2.0

The ultimate analysis consists of determining the mass fraction of the chemical elements in the fuel. This type of analysis is expressed in equation 2.2 (Basu, 2018):

$$C + H + O + N + S + ASH + M = 100\% \tag{2.2}$$

where M is the moisture or humidity ratio in the fuel. Table 2.2 compares the ultimate analysis of some fuel types.

Table 2.2 – Comparison of ultimate analysis of some biomass types (Klass, 1998)

Fuel	C [wt % db]	H [wt % db]	O [wt % db]	N [wt % db]	S [wt % db]	Ash [wt % db]
Pine wood	51.8	6.3	41.3	0.1	0	0.5
Primary biosolids	43.75	6.24	19.35	3.16	0.97	26.53
Kentucky bluegrass	45.8	5.9	29.6	4.8	0.4	13.5

The higher heating value (HHV) may be calculated using correlations based on proximate analysis (equation 2.3) as a function of fixed carbon (FC) [wt % db] and volatile matter (VM) [wt % db] and ultimate analysis (equation 2.4) (Nhuchhen and Afzal, 2017), with the understanding that the correlations for the ultimate analysis are expected to be the most accurate (Sheng and Azevedo, 2005).

$$HHV = 0.1846VM + 0.3525FC \quad [MJ\ kg^{-1}] \tag{2.3}$$

$$HHV = 32.7934 - 0.0053C^2 - 0.5321C - 2.8769H + 0.0608CH - 0.2401N \quad [MJ\ kg^{-1}] \tag{2.4}$$

The HHV can also be measured using calorimetry (Figure 2.4). This consists of housing a sample of biomass fuel in a pressurized oxygen bomb. With the aid of a fuse wire, this sample is then combusted, which releases heat. By knowing the initial mass of the fuel sample and the heat released, the HHV can be calculated by dividing the heat released by the mass of the sample (Basu, 2018). The resulting value of HHV reflects the maximum energy that one can get from the complete combustion of the fuel.

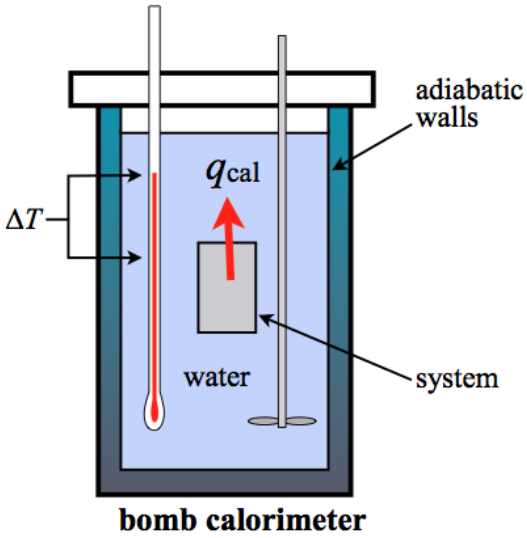

Figure 2.4 – Schematic illustration of a bomb calorimeter (of Texas, 2015).

When biomass is burned in the boiler, the used heat doesn't cool down to the steam condensation temperature. Thus, the heat that was used to evaporate the water present in the fuel is not recovered. For this reason, the useful heat is given by the lower heating value (LHV), which is given by:

$$LHV = HHV - \lambda \left(\frac{9H}{100} - \frac{M}{100} \right) \tag{2.5}$$

where:

λ = latent heat of vaporization of water in the same units as HHV
H = hydrogen content in fuel [wt% wb]
M = moisture content in fuel [wt% wb].

2.1.6 Biomass storage

Storage of biomass in an industrial process may be required, either in long or short term. Biomass storage requires careful planning and associated risks should be taken into consideration.

Fresh bark and wood chips are prone to biological and biochemical decay when piled, leading to a significant increase in temperature that can reach up to 60 $^{\circ}C$ in the first days, and self-ignition may occur when stored for longer than five months or in piles exceeding 8 meters. Additionally, biomass degradation can lead to dry matter losses, which can reach up to 5 % per month (van Loo and Koppejan, 2008).

Dry piles of biomass, when directly exposed to weather conditions, may reabsorb moisture, which reduces its energy content and may increase health risks due to the growth of fungi and bacteria.

Thus, effective storage requires attention to these risks. Temperature and gas emissions to monitor self-ignition risks, indoor storage with natural convection systems for drying or outdoor storage with rain coverage are examples of strategies to mitigate these issues (van Loo and Koppejan, 2008).

2.2 Boiler

Direct-fired boilers are a simple way of converting the chemical bonding energy of biomass into useful thermal energy. This process allows energy to be transferred from the combustion gases to a working fluid, such as water or thermal oil. In this way, we can treat a boiler as a heat exchanger, with a combustion chamber and a region dedicated to heat transfer.

Generally, boilers are rated for a maximum design power output but operate at a partial load. Since boiler efficiency varies with multiple factors, it is necessary to analyze boiler operation under different conditions, including operation at different loads (CIPEC, 2009).

2.2.1 Boiler types

In terms of construction, boilers can be classified as fire-tube, where the hot gases or combustion gases circulate inside the tube bundle or water-tube, where the gases flow outside the tubes. Figure 2.5 illustrates these types of boilers when water is the fluid to be heated, but air or thermal oil can also be used.

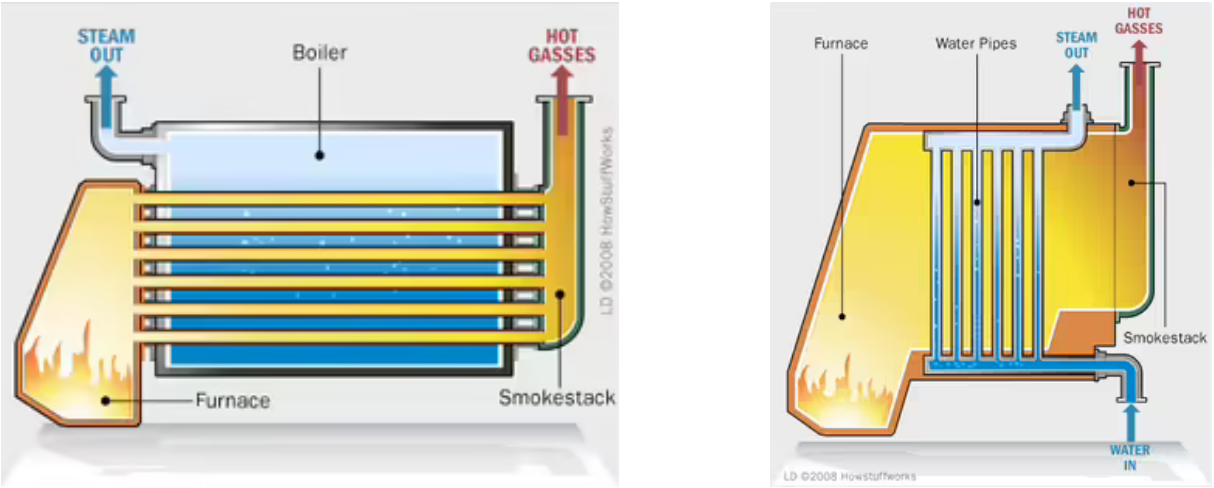

Figure 2.5 – Schematic view of a fire-tube boiler (left) and a water-tube boiler (right) (Marshall Brain, 2023).

2.2.2 Combustion technology in boilers

In industrial plants with boilers of more than 100 kW, the fuel supply is supported by control systems and mechanical or pneumatic feed systems (van Loo and Koppejan, 2008).

These boilers have different combustion technologies depending on the desired application, such as fixed bed combustion, fluidized bed combustion (bubbling and circulating) and pulverized fuel combustion (Figure 2.6). These types can be distinguished according to the type of flow that occurs in the furnace.

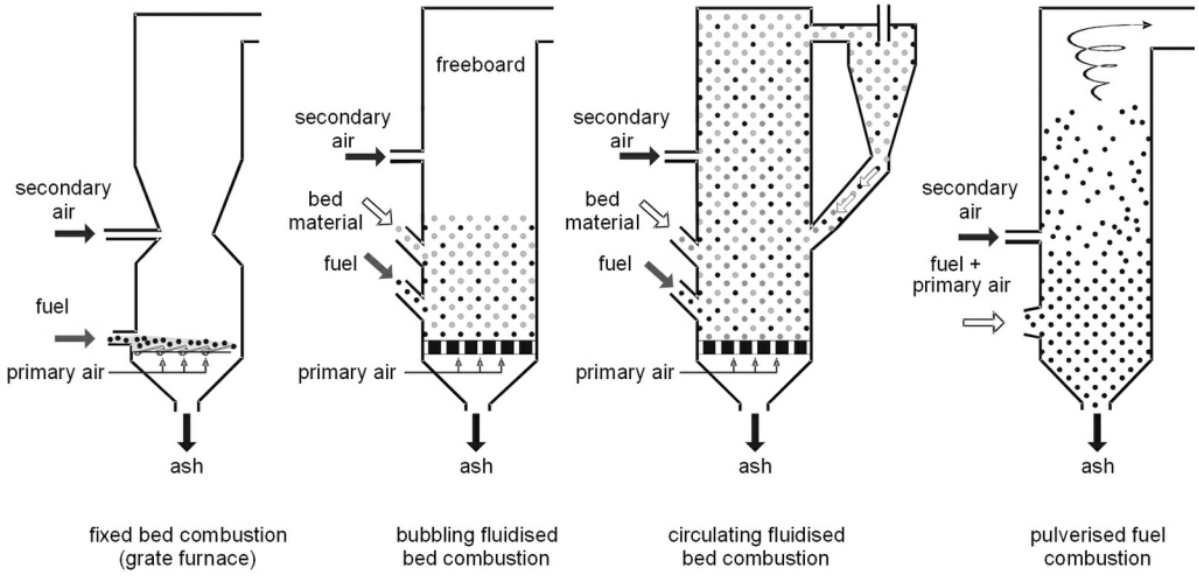

Figure 2.6 – Schematic view of different boiler combustion technologies (van Loo and Koppejan, 2008).

In the case of fixed bed combustion, the fuel is stationary in a bed or a grate that can be fixed or dynamic. A flow of air is introduced at the bottom of the bed, ensuring combustion at a regulated temperature (van Loo and Koppejan, 2008).

Fluidized bed boilers are the best technology for burning fuels of poor quality, high ash content and low calorific value (Saidur et al., 2011). In these furnaces, the fuel is added to a bed of hot solid particles. This mixture, when hit by an ascending air flow, reaches a state of fluidization with typical properties of a fluid. This process allows for a higher heat transfer rate and lower operating temperatures, which improves the combustion process efficiency (Crawford, 2012).

The pulverized bed technology relies on the combustion of finely ground biomass particles suspended in an upward-flowing air or gas steam. The biomass particles should be less than 1 mm in size to achieve a uniform and thorough burning process, ensuring a high degree of combustion control and efficiency (Amamoto et al., 2019).

2.2.3 Boiler efficiency

Boiler efficiency is based on several parameters of operation, including load, fuel, temperatures, flue gas and air/fuel mixture. The overall boiler efficiency results in the ratio of the useful heat delivered by the boiler and the supplied heat to the boiler by fuel, which is the direct method for efficiency evaluation and is represented by Equation 2.6 (de Pinho, 2016).

$$\eta_{boiler} = \frac{Useful\ Heat}{Fuel\ Heat}\ [\%] \tag{2.6}$$

Where useful heat can be referred to the heat gained by the operating fluid and is calculated by the flow rate of the fluid $(\dot{m})$ multiplied by the enthalpy difference between the output (h_{out}) and input (h_{in}) and fuel heat is calculated by the multiplication of fuel flow $(\dot{m}_{fuel})$ by it's HHV in boilers where water vapor energy is reused (condensation boilers) or by LHV when water vapor energy is lost in flue gas. Such that:

$$Useful\ Heat = \dot{m} \cdot (h_{out} - h_{in}) \tag{2.7}$$

$$Fuel\ Heat = \dot{m} \cdot HHV/LHV \tag{2.8}$$

This method requires measurement of fuel flow and laboratory analysis of its heating value being the fuel gaseous, liquid or solid. For the heat output, it is required flow and temperature meters with a pressure sensor for flow correction.

Combustion efficiency can also be investigated by measuring O_2 content in the flue gas. The relation between combustion efficiency and O_2 content in the flue gas is given by a chart (Figure 2.7). A high amount of O2 present in the flue gas indicates that too much air is being used in the mixture. Thus, the combusting is becoming inefficient and the heat output is reduced.

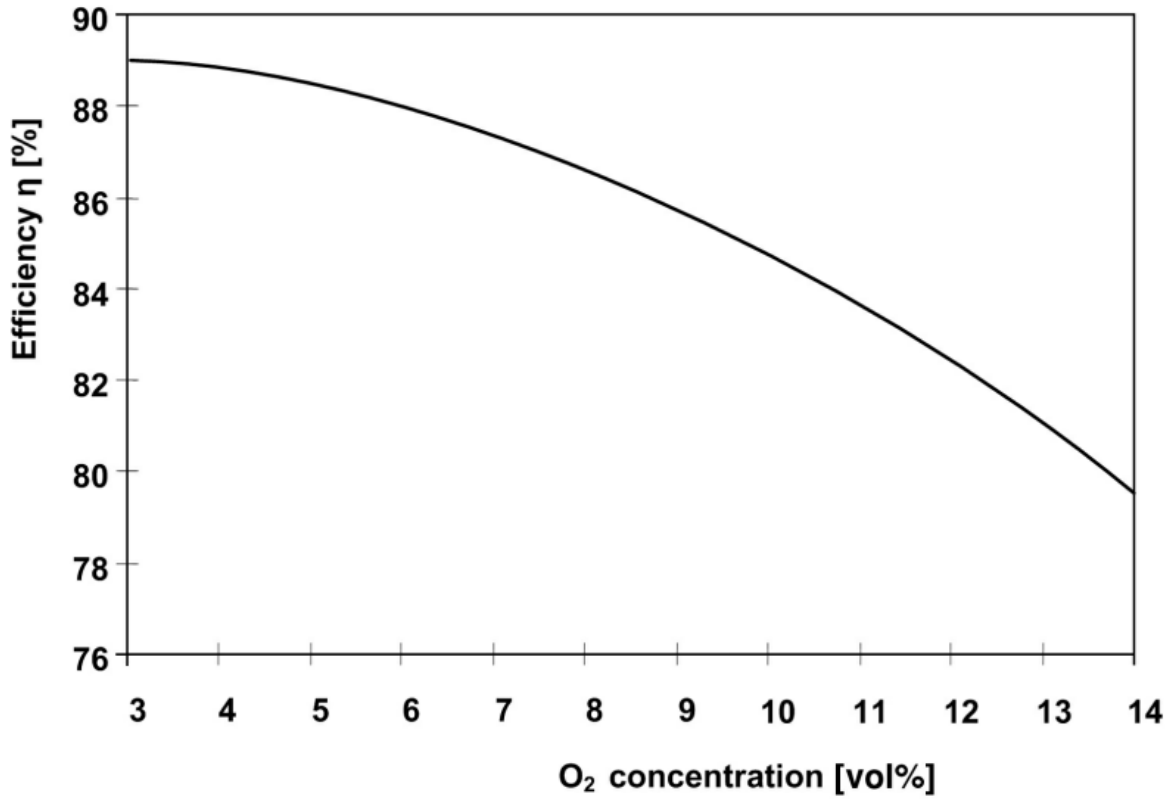

Figure 2.7 – Oxygen content in the flue gas and combustion efficiency relation (van Loo and Koppejan, 2008).

2.3 Dryer

One of the most crucial processing phases in the production of wood composites is drying. The fresh cut wood contains a large amount of water and it needs to be dried. This water extraction is essential to improve the mechanical properties of the wood. Drying improves stability, reducing the risk of warping, cracking, biological decay, and fluctuations in dimensions. Beyond these mechanical benefits, drying also makes transportation and handling more cost-effective as removing moisture reduces the overall weight of the wood.

Wood can be dried through three different methods. The first involves the usage of a hot fluid, known as convective drying. In this process, the hot fluid transfers heat to the wood, increasing the water molecules' evaporation rate. The second method is vacuum drying, which is carried out at reduced atmospheric pressure conditions (Niemz et al., 2023). The third is solar drying, which uses solar energy to heat wood, offering a cost-effective and environmentally friendly option.

In the case of the convective drying, energy analysis can be made by applying equation 2.9 (Zhou et al., 2010):

$$\dot{Q} = \dot{m} \times C_u \times \Delta T \tag{2.9}$$

where, $\dot{Q}$ is the thermal energy consumed for drying [W], $\dot{m}$ is the hot fluid flow [kg/s], C_u is

the specific heat of the fluid [J/(kg·K)] and ΔT is the fluid temperature difference at the dryer inlet and outlet.

2.4 Press

In many industrial processes, high-temperature compaction is required to form materials such as wood composites, rubber or plastics. One solution to meet high operating temperatures is the use of thermal fluids.

Thermal fluids are synthetic fluids with heat transfer properties, stability and safety best suited to operations at temperatures above 220 ºC where the use of steam or pressurized water is no longer suitable (de Pinho, 2016).

The press reaches its operating temperature through heating mechanisms such as thermal oil. The heat carried by the thermal oil is transferred to the plate by a coil installed inside the plate itself. This heating system guarantees a uniform temperature across the entire surface.

Chapter 3

PROBLEM DESCRIPTION

3.1 Sonae Arauco - OH

Sonae Arauco's industrial plant in Oliveira do Hospital (OH) is dedicated to the production of Particle Board (PB) and Melamine Faced Chipboard (MFC) (Figure 3.1).

Figure 3.1 – PB (left) and MFC (right) products.

The plant was founded in 1968 as Agloma, initially for the production of PB and when Sonae acquired Algoma in 1984, a new coating line was installed.

The factory currently covers an area of 25 hectares, employs around 230 people and has a production capacity of 1250 m^3/day of PB and 805 m^3/day of coating.

Vyncke's current biomass thermal energy plant was installed in 2008, supplying hot gases and heated thermal oil for the manufacturing process.

3.2 OH thermal energy plant

The OH biomass thermal energy plant produces hot gases resulting from the combustion process in its furnace. The hot gases directly feed two wood particle dryers and indirectly feed the continuous line, impregnation and coating presses via a thermal oil heated in a heat exchanger. The manufacturer specifies a maximum output energy rate of 32.6 MW for the hot gas and 13.1 MW for the thermal oil, totalling 45.7 MW for the thermal energy plant. Figure 3.2 shows a schematic illustration of the thermal energy plant.

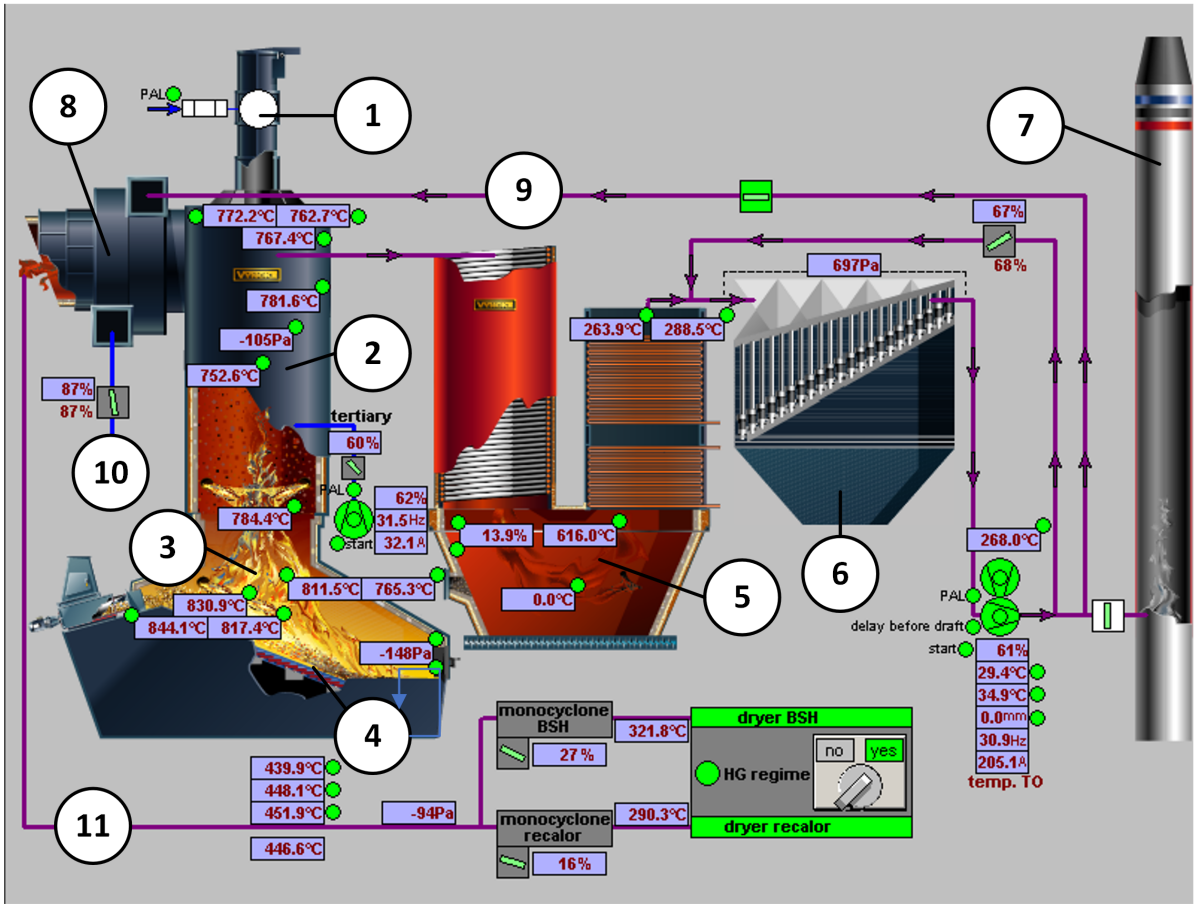

(1) Emergency chimney. (2) Post combustion chamber - turbix. (3) Combustion room. (4) Dynamic water cooled step grate. (5) Thermal oil heat exchanger. (6) Dust collector. (7) Start up chimney. (8) Mixing chamber. (9) Flue gas. (10) Mixing chamber air intake. (11) Hot gas for dryers.

Figure 3.2 – OH thermal energy plant schematic view (control software).

3.2.1 Boiler

The boiler was designed to operate with bark, solid wood waste, black dust and white dust, with the last two being rejects of the manufacturing process. The manufacturer *Vyncke* specifies the characteristics of the fuel to be used (Table 3.1).

Bark and solid waste are fed into the furnace for grate combustion. The 61 m^2 grate can handle a fuel flow rate of 24000 kg/h through two fuel launch systems (Figure 3.3) with five feeding screws each. The feeding speed is controlled by pre-calculated settings depending on the desired boiler load.

Table 3.1 – Boiler fuel specification

Fuel	Bark and wood residues mix	Black dust	White dust
Nominal LHV wb [kJ/kg]	9204.8	16737	16736
Minimal LHV wb [kJ/kg]	7949.6	-	-
Maximal LHV wb [kJ/kg]	11715.2	-	-
Nominal moisture content wb [wt. %]	43	-	-
Minimal moisture content wb [wt. %]	32	-	-
Maximal moisture content wb [wt. %]	49	-	-
Maximum ash content db [%]	8	8	8

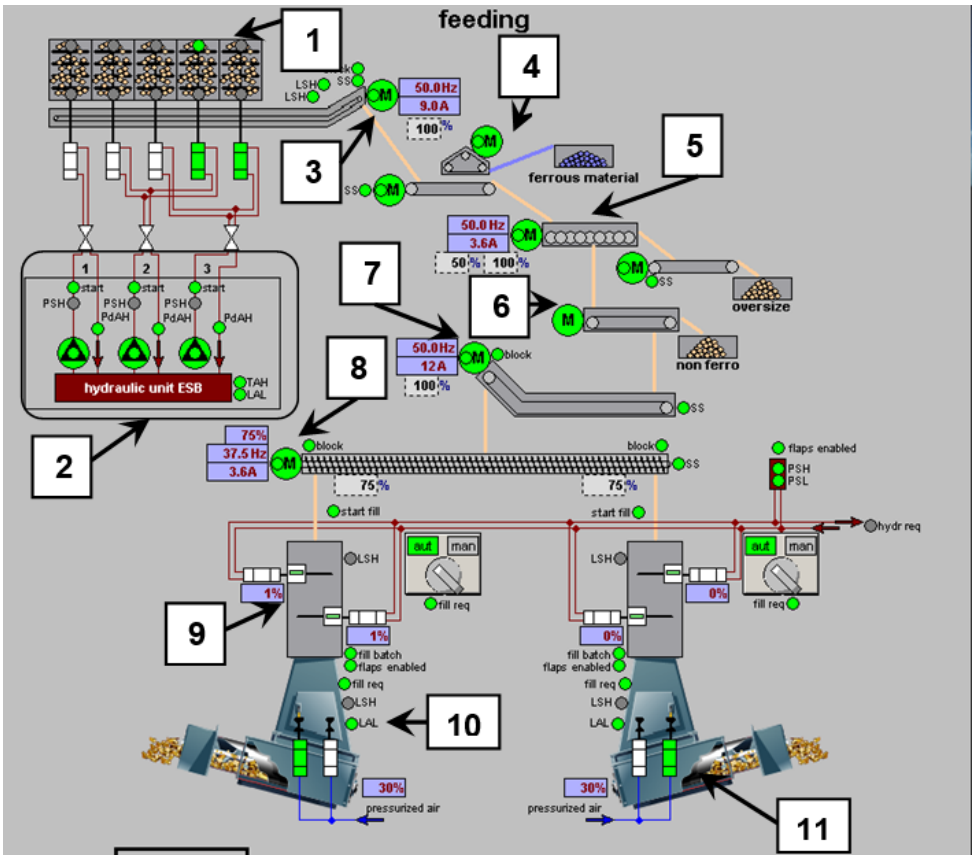

(1) Silo with moving floor. (2) Fuel hydraulic group. (3) Belt conveyor. (4) Ferrous materials over belt. (5) Disk separator. (6) Non-ferrous separator. (7) Redler for left/right screw separator. (8) Left/right separator for fuel feeding system. (9) Air flap. (10) Left fuel feeding system. (11) Right fuel feeding system.

Figure 3.3 – Boiler fuel launch system schematic view (control software).

Pulverized combustion is carried out by injecting black dust at 4 points above the grate and white dust at 2 points in a combustion chamber above the furnace called *turbix*. The injection of dust is made with air for better combustion and the airflow is regulated by flaps. Since the combustion of the dust is guaranteed by the grate flames, the control system only allows dust to be injected when a sufficient temperature is measured in the furnace. The injectors have

a maximum capacity to guarantee a dust flow of 750 kg/h. The hot gases leave the combustion chamber at a temperature of 920 °C.

The boiler grate is water cooled and the lost heat to water is used to heat the combustion primary and secondary air intake through a heat exchanger. The combustion works with excess air and the mixture is controlled by the air intake fans and air duct flaps depending on the boiler load.

3.2.2 Thermal oil heater

The thermal oil in use at the plant is BP Transcal N, whose material properties vary with temperature. Density and specific heat will be the relevant properties for the energy balance and can be calculated as a function of its temperature (de Pinho, 2016):

$$\rho = 879.41 + 0.5992T \tag{3.1}$$

$$C_p = \frac{4.187}{\sqrt{\rho/1000}}(0.403 + 0.00081 \cdot T) \tag{3.2}$$

where:

ρ = density $[kg/m^3]$
T = thermal oil temperature $[^\circ C]$
C_p = thermal oil specific heat $[kJ/(kgK)]$.

The thermal oil specified flow of 580 m^3/ h is heated in the thermal oil heat exchanger (Figure 3.4) that comprises one radiation part (Coil) and one convection part (ECO). The helical coil cools the hot gases from 925 to 800 °C and the tubular heat exchanger further cools the gases to 400 °C. The primary thermal oil circuit then includes pumps, valves, control equipment and one emergency cooling circuit. The control of thermal oil temperature is made by a PID regulation of the flue gas fan situated after the heat exchanger that keeps thermal oil at the set point temperature.

Thermal oil returns from the consumers through three pumps (one is always at stand-by) then flows through the heat exchanger and is supplied to the consumers through four pumps (two are always at stand-by).

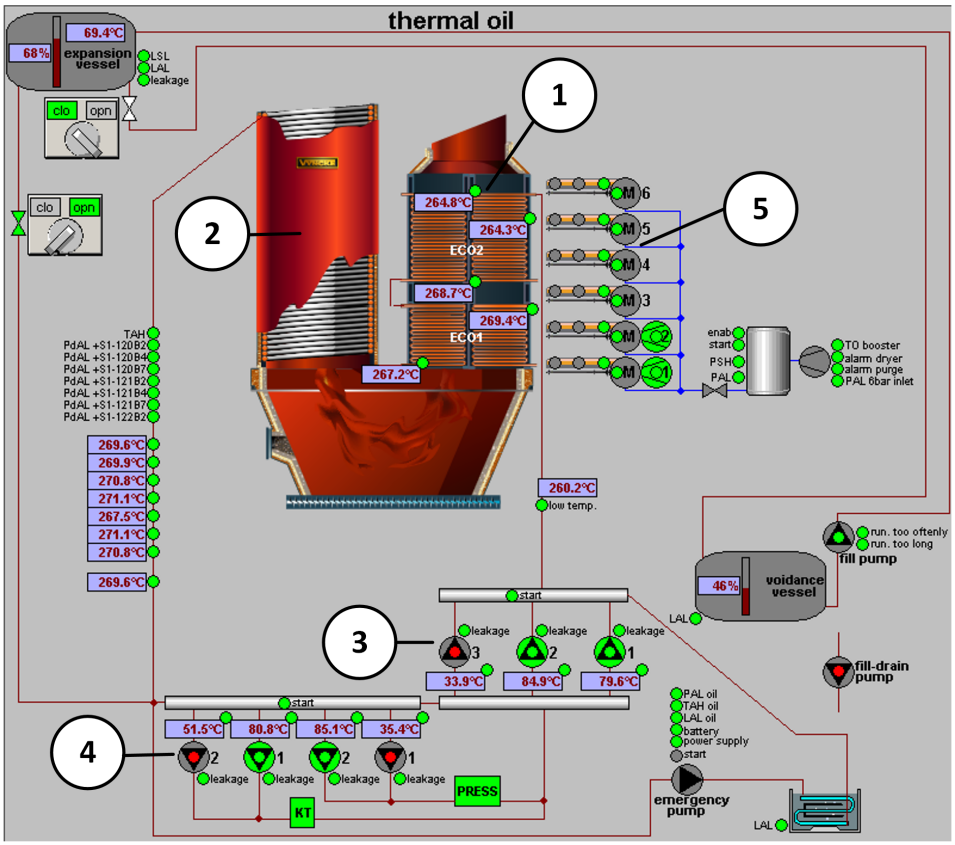

(1) ECO. (2) Coil. (3) Return circuit pumps. (4) Supply circuit pumps. (5) Scoot blowers.

Figure 3.4 – Thermal oil heat exchanger schematic view (control software).

3.2.3 Dust collector

When thermal oil is used and the dryers are not in operation, the hot gases are no longer needed and are released into the atmosphere via a chimney. These hot gases contain dust and ash that must be separated in a dust collector. This dust collector consists of several cast iron cyclones where the hot gases are evenly distributed. The heavier particles are hurled against the outer wall by centrifugal force and glide downwards a collecting funnel where an ash bin collects the particles.

3.2.4 Mixing chamber

The gases coming from the dust collector are mixed with combustion gases extracted from a second exit on the *turbix* and with ambient air. In this process, the hot gases mixture outlet temperature is about 550 °C.

3.3 Fuel flux

The fuel used in the thermal energy plant comes from external suppliers and process rejects.

Biomass is acquired in the form of chips, chip fines, bark and chopped forest biomass. When this type of biomass arrives at the plant, it is weighted and stored exposed to weather and is therefore submitted to moisture content analyses several times a day. Prior to injection into the boiler, this fuel passes through a disk separator, which rejects particles larger than those specified in Table 3.1 and a ferrous materials separator.

Biomass from process rejects results in black dust and white dust. Black dust origins in waste from the process of incorporation of recycled particles in the recycled tower and from the separation and refining of particles prior to the continuous line on screeners and in the Algaier system. White dust is referred to as waste from sanding and trimming of particle boards. Black dust is weighted, while the mass of white dust is determined through calculations based on a over-thickness loss factor.

This flux is shown in Figure 3.5.

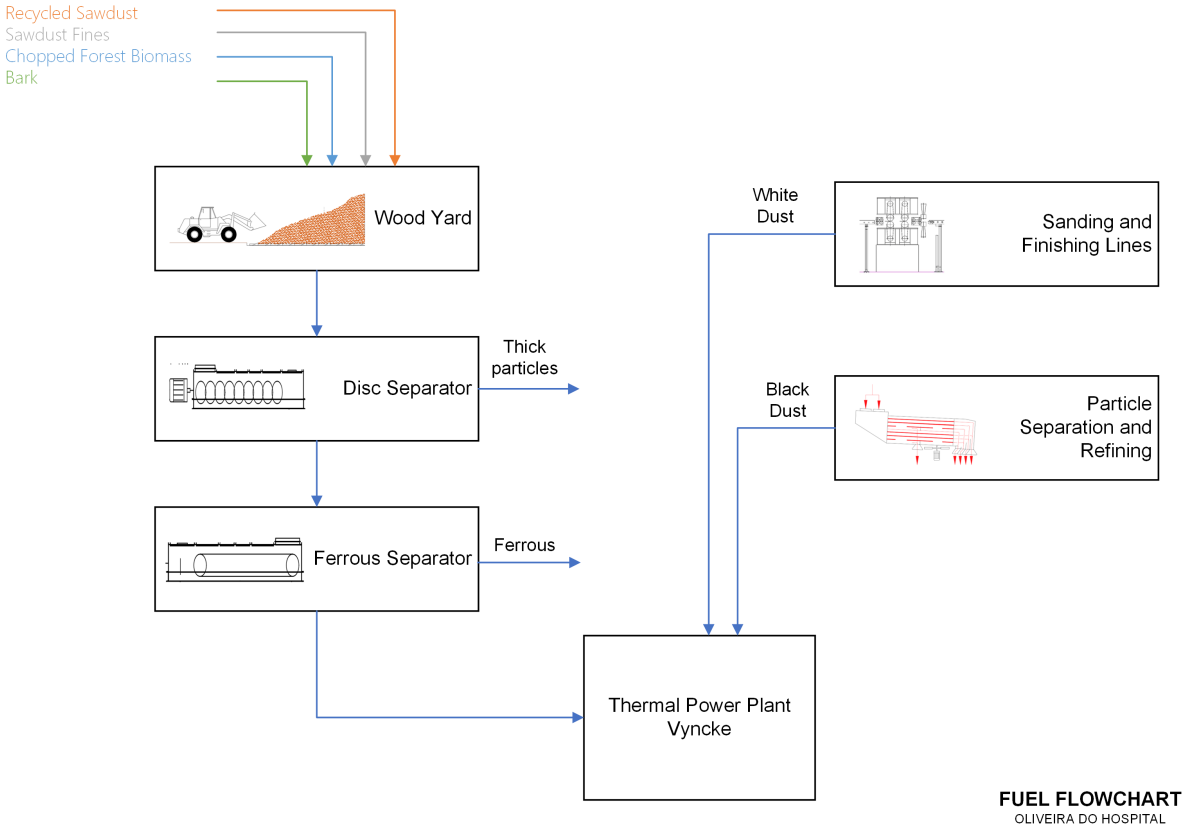

Figure 3.5 – Fuel flowchart.

3.3.1 Fuel characterization

Analyses of each type of biomass were conducted by an external laboratory and the results are shown in Table 3.2.

Table 3.2 – Fuel analysis results

Property	**Recycled wood chips**	**Sawdust fines**	**Chopped forest biomass**	**Bark**	**White dust**	**Black dust**	**Obs.**
Carbon content db [wt.%]	47.39	45.00	45.10	51.10	45.30	45.60	Ultimate analysis (ISO 16948:2015)
Hydrogen content db [wt.%]	6.17	5.80	5.50	6.10	5.80	6.30	
Nitrogen content db [wt.%]	2.84	2.05	2.10	0.30	5.80	1.40	
Sulphur content db [wt.%]	0.07	0.18	0.05	0.03	0.10	0.09	
Oxygen content db [wt.%]	38.20	35.55	36.20	34.40	39.20	37.80	Calculus (ISO 16993:2015)
Moisture content wb [wt.%]	35.41	27.60	52.40	45.7	4.60	3.10	Gravimetry (ISO 14774:2009)
Ash content db [wt.%]	4.67	11.30	9.90	8.10	2.70	8.70	Gravimetry (ISO 14775:2009)
HHV db [MJ/kg]	19.09	17.91	18.32	20.05	19.37	18.92	Calorimetry (EN 14918:2009)
LHV db [MJ/kg]	17.82	16.15	17.10	18.73	18.10	17.55	
LHV wb [MJ/kg]	10.53	11.37	6.86	9.05	17.15	15.93	

Analyzing the results, one can see a decrease in wet basis LHV as the moisture content increases. This phenomenon is particularly relevant when considering an annual period in which the biomass reflects the natural fluctuations in the relative humidity of the atmospheric air. The

analyses carried out at the factory on the biomass purchased and the relative humidity values recorded over a period of one year are related in Figure 3.6.

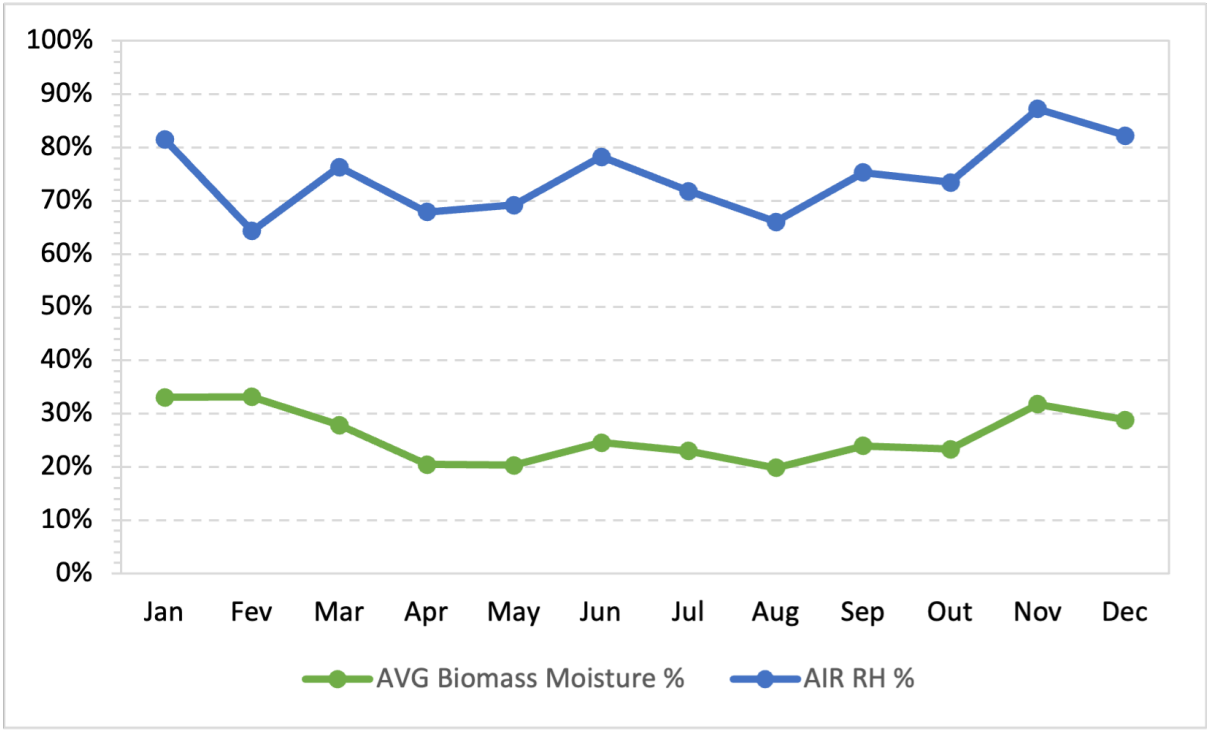

Figure 3.6 – Relation between biomass moisture and air relative humidity.

3.4 Thermal energy consumers

3.4.1 Dryers

Drying the wood particles is needed to reduce moisture, ensuring that the final product has proper characteristics and quality. This process is ensured by two dryers, BSH and Recalor. These two rotary drum-type dryers, with an inner labyrinth, use heat from the combustion gases coming from the thermal energy plant. The wet particles are thrown through a sluice in the drying chamber and then into the drying drum. The amount of time that the particles remain in the drum can be regulated by the number of revolutions of the drum, it thus provides a way of controlling the moisture content of the particles. After having passed the drum dryer, the now dry wood particles are separated from the cooled and moist hot gases in cyclone collectors.

The technical characteristics of this equipment are provided by their manufactures (Table 3.3).

Table 3.3 – Dryers specifications

Dryer	Recalor	BSH
Thermal power [MW]	19.2	20
Capacity db [kg/h]	18 900	22 000
Hot gases inlet temperature [°C]	450	500-520
Hot gases outlet temperature [°C]	110	110

The plant's control software (Figure 3.7) enables the regulation of particle moisture by adjusting the particle flow rate, air dumpers positions at the dryer inlet and air/fuel ratio in the combustion room. Additionally, the software records the temperature of gases and moisture content of the wood particles at the inlet and outlet of the dryers.

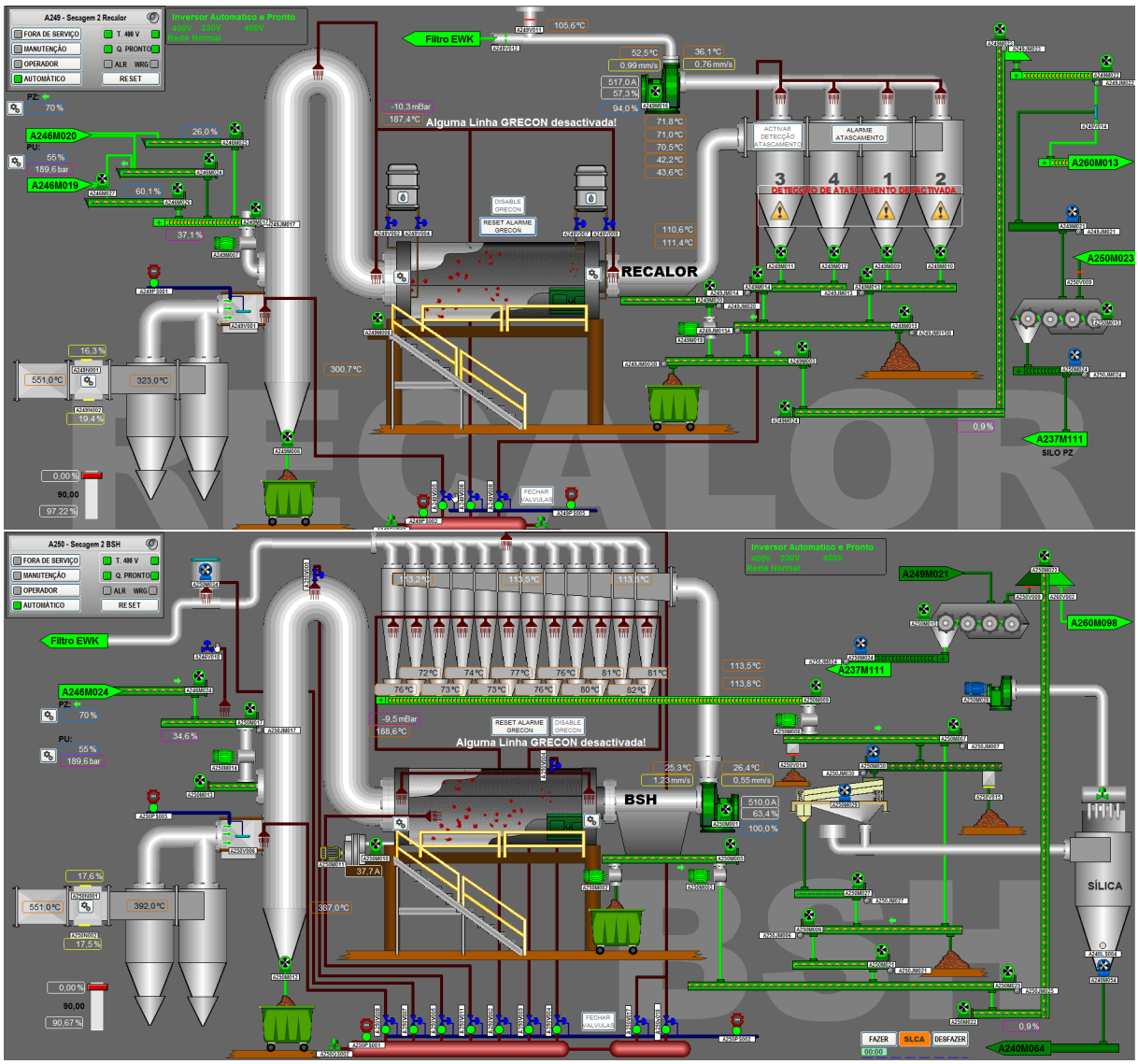

Figure 3.7 – Dryers control software.

3.4.2 Continuous line press

After drying, separating and refining the wood particles, they are processed in the *Siempelkamp* continuous line to transform them into particle boards. The continuous line involves several operations:

- gluing;
- formation;
- pre-pressing;
- hot pressing;
- cutting.

The process of hot pressing involves the continuous compaction of a mattress of particles with the introduction of heat, resulting in the formation of a compact particle board (Figure 3.8).

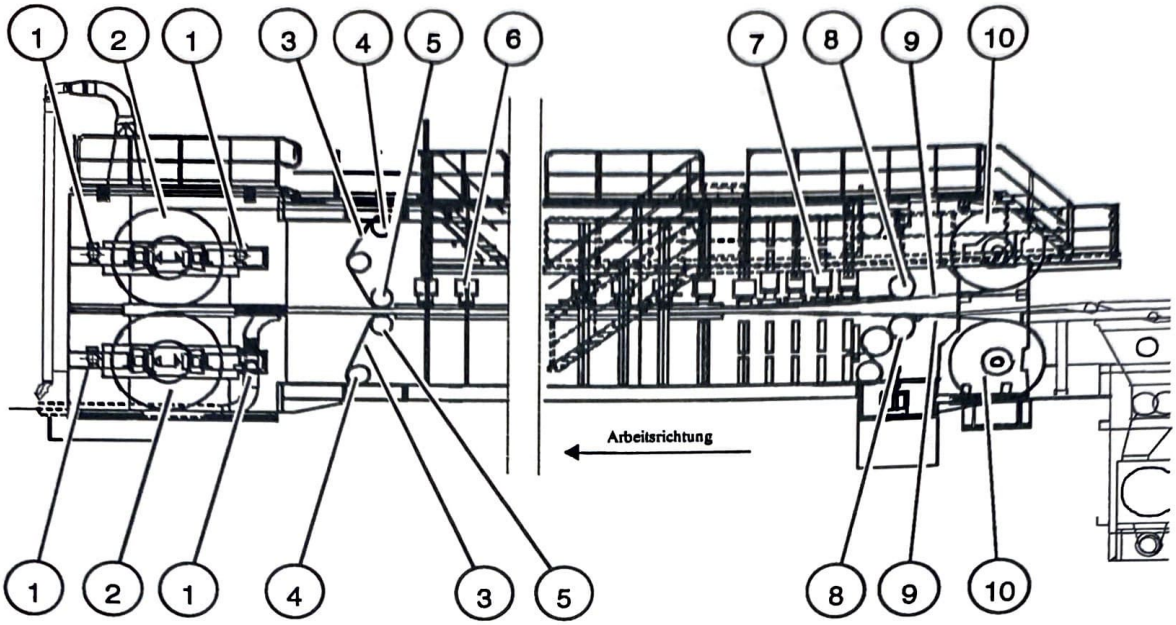

(1) Main drive motors. (2) Exit rolls. (3) Rolling bar chain. (4) Rolling bar chain tensioner. (5) Chain drive motors. (6) Pressing cylinder. (7) Entrance adjustment (with displacement and adjustment cylinders). (8) Diverting roller drivers. (9) Steel belt. (10) Entrance rolls.

Figure 3.8 – *ContiRoll*® hot press.

The pre-pressed particles are compacted inside the hot press by two heated steel belts. The compression force comes from hydraulically driven pressing cylinders. The heat is supplied by thermal plates filled with thermal oil that transfer heat in five stages (225 to 180 $^{\circ}C$) to the steel belt. The continuous line press manufacture specifies a heating power of 5.8 MW.

3.4.3 Impregnation lines

This section involves two lines, VITS1 and VITS2, where bought decorative paper is impregnated with resins (Figure 3.9). The paper is first passed trough a solution of urea resins and formaldehyde. Following this bath, the paper passes through one drying oven in VITS1 and a set of two ovens in VITS2, where the drying air is heated by the thermal oil through a heat exchanger. The subsequent step involves immersing the paper in a melamine resin bath and then drying in another set of four drying rooms until the paper reaches a moisture content of 5 to 7 %. After the drying oven, the paper is cooled by forced convection with ambient air and is cut with a guillotine. The stacked paper is then stored.

The heating power specifications for each impregnation line, as provided by the manufacturer, are shown in Table 3.4.

Table 3.4 – Impregnation lines thermal power specifications

Line	VITS1	VITS2
Power [MW]	1.1	1.1

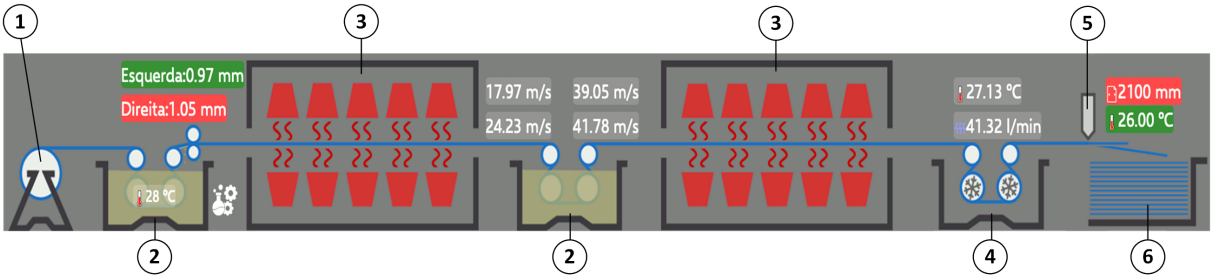

(1) Unwinder. (2) Resins bath. (3) Drying oven. (4) Chilling rollers. (5) Guillotine. (6) Stacking.

Figure 3.9 – Impregnation line.

3.4.4 Melamine coating lines

To apply the impregnated paper to the surfaces of particle boards from the continuous line press and from external manufacturers, there are four lines: BP6, BP7, BP8 and BP9.

The first step of these lines is to form three layers: under paper, board and upper paper. Then, this group of layers goes to the short cycle hot hydraulic press (Figure 3.10) with an upper and under plate, heated by thermal oil to temperatures from 175 to 205 °C. The pressure and temperature of the press plates cause the resins impregnated in the paper to react and permanently adhere to the particle board.

After pressing, the excess paper is removed with scrapers and the board is cut with a cross-cut saw. Finally, the board is cleansed, packed and stored for shipping.

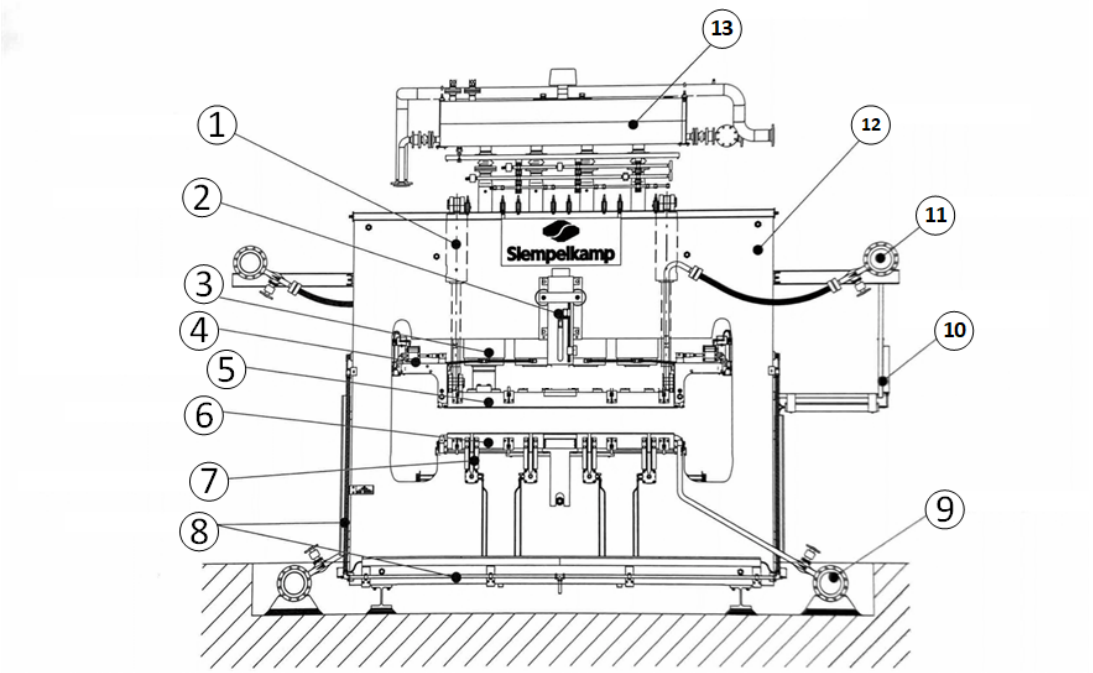

(1) Lifting cylinder. (2) Upper hot plate guide. (3) Compressing cylinder. (4) Upper sheet tensioner. (5) Upper hot plate. (6) Under hot plate. (7) Under sheet tensioner. (8) Leaking oil pipe. (9) Under heating circuit. (10) Pneumatic plate tensioner. (11) Upper heating circuit. (12) Frame sheet. (13) Oil reservoir.

Figure 3.10 – *Siempelkamp* BP8 short cycle press (front view).

The short-cycle presses manufactures specify the operating thermal powers (Table 3.5).

Table 3.5 – Pressing lines thermal power specifications

Line	BP6	BP7	BP8	BP9
Manufacture	Siempelkamp	Wemhomer	Siempelkamp	Whemhomer
Thermal power [kW]	255	640	755.95	697.8

3.5 Thermal energy balance model

This section aims to develop the thermal energy balance model for the thermal energy plant and for the thermal energy users.

3.5.1 Thermal energy plant

The flows that will be considered in the balance of the combustion chamber of the thermal energy plant are shown in Figure 3.11. The existing flows are: biomass (1), primary air (2), secondary air (3), tertiary air (4), flue gases (5,6,7), air entering the mixing chamber (8), the air and flue gases mixture (hot gases) (9) and the heat lost to thermal oil ($\dot{q}_{to}$).

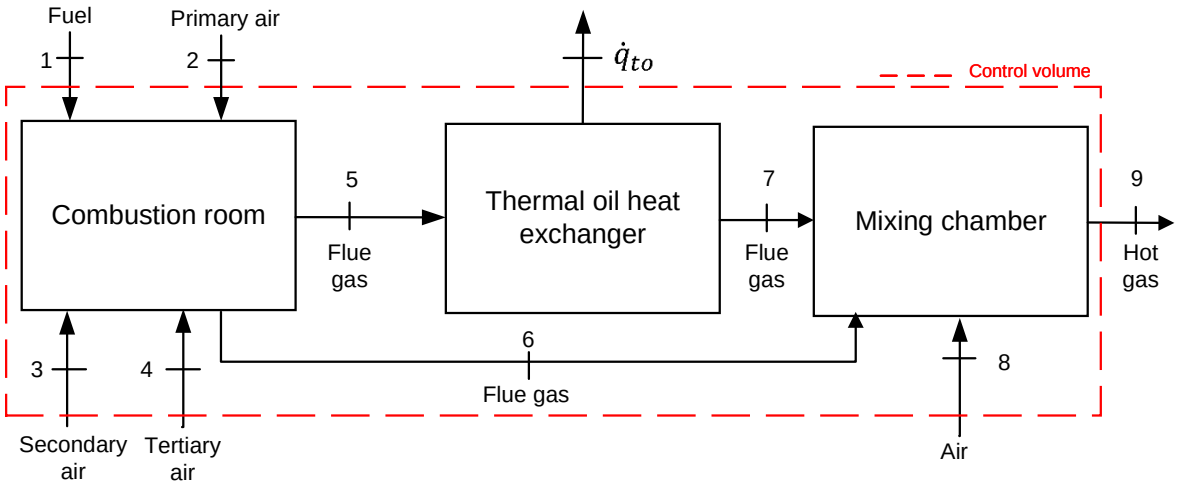

Figure 3.11 – Thermal energy plant diagram.

The mass balance applyed to the control volume of the thermal energy plant is given by the following equation:

$$\dot{m}_1 + \dot{m}_2 + \dot{m}_3 + \dot{m}_4 + \dot{m}_8 = \dot{m}_9 \tag{3.3}$$

Applying the first law of thermodynamics to the same control volume and disregarding variations in kinetic and potential energies, one can get the following steady-state equation for the energy balance:

$$\dot{m}_1 LHV + \dot{m}_2 h_2 + \dot{m}_3 h_3 + \dot{m}_4 h_4 + \dot{m}_8 h_8 = \dot{m}_9 h_9 + \dot{q}_{to} \tag{3.4}$$

The hot gases will then exchange heat with thermal oil. Figure 3.12 illustrates the flows in the thermal oil heat exchanger, which consists of a heat transfer zone by radiation (coil) and another by convection (eco).

The thermal energy rate transferred to the thermal oil can be calculated using Equation 3.5.

$$\dot{q}_{to} = \dot{V}_{to}\, \rho_{to}\, C_{p_{to}}\, (T_{out} - T_{in}) \tag{3.5}$$

Where:

$\dot{q}_{to}$ = thermal energy rate transferred to thermal oil [kW]
$\dot{V}_{to}$ = pumped thermal oil volumetric flow rate [m^3/ s]
ρ_{to} = thermal oil density [kg/m^3]
$C_{p_{to}}$ = thermal oil specific heat [kJ/(kg·K)]
T_{out} = thermal oil supply temperature [°C]
T_{in} = thermal oil return temperature [°C].

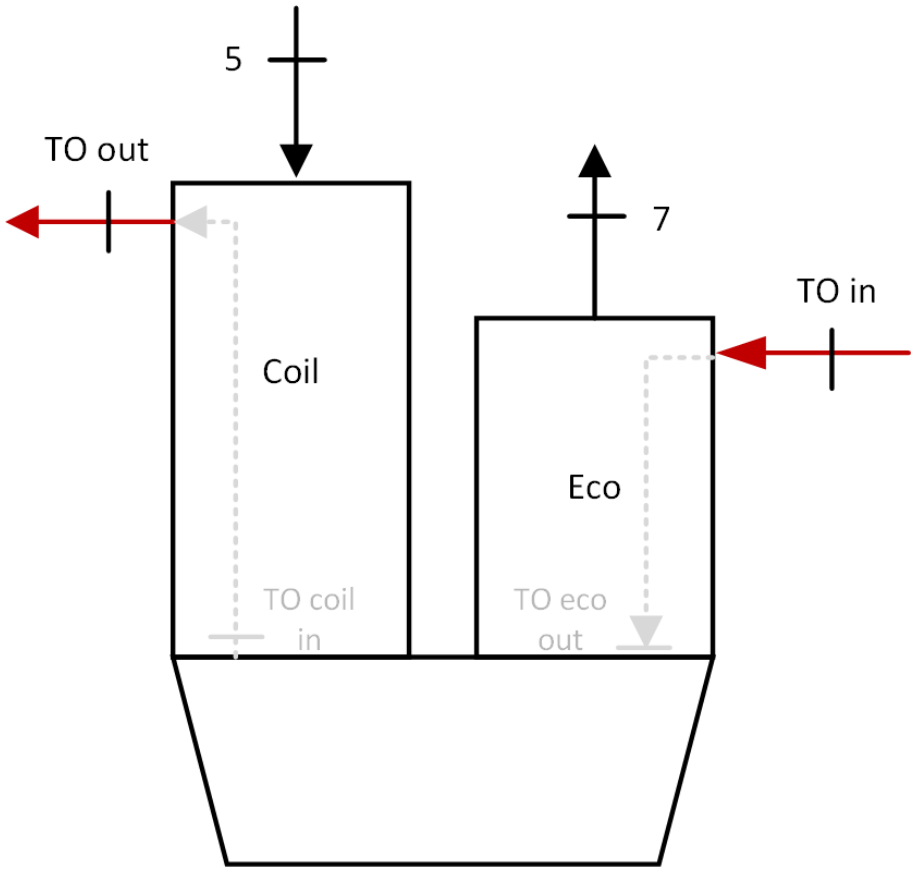

Figure 3.12 – Thermal oil heat exchanger flux diagram.

3.5.2 Hot gas users

The dryers use the flow of hot gases from the thermal energy plant, specified by (7) in Figure 3.11, which after splitting, merges with an ambient air flow in each monocyclone. The hot gas flux is possible due to the fan installed at the outlet of each dryer. This process is illustrated in Figure 3.13.

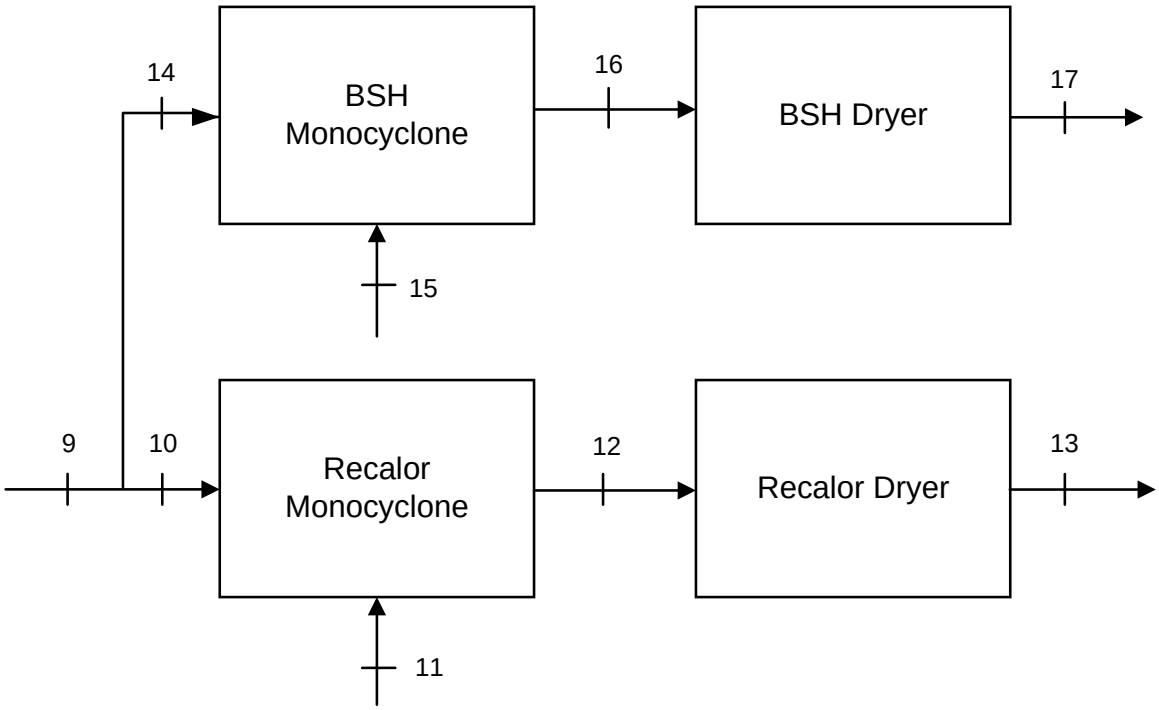

Figure 3.13 – Dryers diagram.

The mass balance applied to two control volumes enclosing each set of monocyclone and dryer is given by in Equations (3.6) and (3.7).

$$\dot{m}_{10} + \dot{m}_{11} = \dot{m}_{13} \tag{3.6}$$

$$\dot{m}_{14} + \dot{m}_{15} = \dot{m}_{17} \tag{3.7}$$

The energy balance applied to each set of monocyclone and dryer results in Equations (3.8) and (3.9).

$$\dot{m}_{10}h_{10} + \dot{m}_{11}h_{11} = \dot{Q}_{Rec} + \dot{m}_{13}h_{13} \tag{3.8}$$

$$\dot{m}_{14}h_{14} + \dot{m}_{15}h_{15} = \dot{Q}_{BSH} + \dot{m}_{17}h_{17} \tag{3.9}$$

Since the purpose of these dryers is to dry wood particles, the useful energy to this process is the one needed to evaporate the excess water. The energy rate required to dry a mass flow of wet wood particles is given by the sum of the sensible heat required to heat the wood particles to the water evaporation temperature with the latent heat required to evaporate the water (Equation 3.10).

$$\dot{q}_{dry} = \dot{m}_{wood}(W_i - W_f)[C_{p_w}(T_{evap} - T_{w_i}) + \lambda] \tag{3.10}$$

Where:

$\dot{q}_{dry}$ = total energy rate required to evaporate water from wood particles [kW]
$\dot{m}_{wood}$ = mass flow rate of wood [kg/s]
C_{p_w} = specific heat of water [kJ/(kg·K)]
T_{evap} = evaporation temperature of water [K]
T_{w_i} = initial wood particles temperature [K]
λ = latent heat of vaporization of water [kJ/kg]
W_i = initial moisture content [%]
W_f = final moisture content [%].

3.5.3 Thermal oil users

These equipment uses thermal oil heated in the heat exchanger of the thermal energy plant (Figure 3.12). Accounting for the thermal energy used involves considering the mass flux of thermal oil given by the circuit pumps and its enthalpy difference at the inlet and outlet of the consumer.

3.5.3.1 Continuous line press

The continuous line press (Figure 3.14) is equipped with five heating circuits for each heating stage. As each circuit is served by a dedicated pump with an electronic speed variator (ESV), we can analyse them independently (Circuit n).

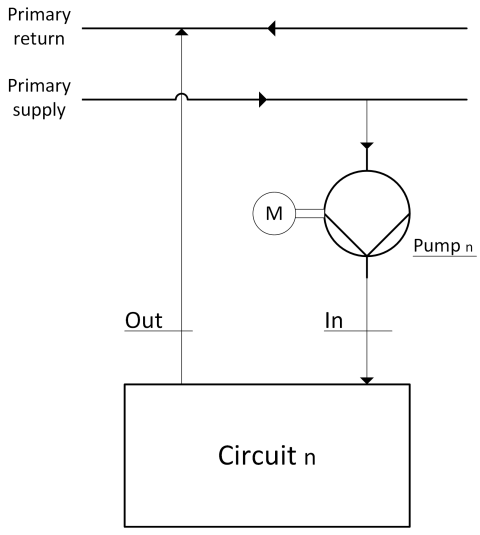

Figure 3.14 – Simplified schematic view of a continuous line press heating circuit.

The total thermal energy rate of the continuous line press will be the sum of the energy usage by each heating circuit (Equation 3.11).

$$\dot{q}_{clp} = \sum_{n} \dot{V}_n \rho_{to_n} C_{p_{to_n}} (T_{in_n} - T_{out_n}) \tag{3.11}$$

Where:

$\dot{q}_{clp}$ = total thermal energy rate usage by the continuous line press [kW]
$\dot{V}_n$ = pumped thermal oil volumetric flow rate of circuit n [m^3/ s]
ρ_{to_n} = thermal oil density at average temperature of circuit n [kg/m^3]
C_{p_n} = specific heat of the thermal oil at average temperature of circuit n [kJ/(kg·K)]
T_{in_n} = thermal oil temperature at the inlet of the circuit n [K]
T_{out_n} = thermal oil temperature at the outlet of the circuit n [K]

3.5.3.2 Impregnation lines

The two impregnation lines are equipped with ovens where air is heated with thermal oil. Each oven features a dedicated pump to regulate the air temperature effectively.

The total thermal energy consumption rate of $VITS_i$ will be given by the sum of the energy consumption rate of each circuit n (Equation 3.12).

$$\dot{q}_{VITS_i} = \sum_n \dot{V}_n \rho_{to_n} C_{p_{to_n}} (T_{in_n} - T_{out_n}) \tag{3.12}$$

Where:

$\dot{q}_{VITS_i}$ = total thermal energy rate usage by VITS i [kW]
$\dot{V}_n$ = pumped thermal oil volumetric flow rate of circuit n [m^3/ s]
ρ_{to_n} = thermal oil density at average temperature of circuit n [kg/m^3]
$C_{p_{to_n}}$ = specific heat of the thermal oil at average temperature of circuit n [kJ/(kg·K)]
T_{in_n} = thermal oil temperature at the inlet of the circuit n [K]
T_{out_n} = thermal oil temperature at the outlet of the circuit n [K].

3.5.3.3 Melamine coating lines

Each coating press BP_n is equipped with dual circuits for each heating plate. These circuits are individually connected to the primary thermal oil supply, with each circuit having its own dedicated pump (Figure 3.15).

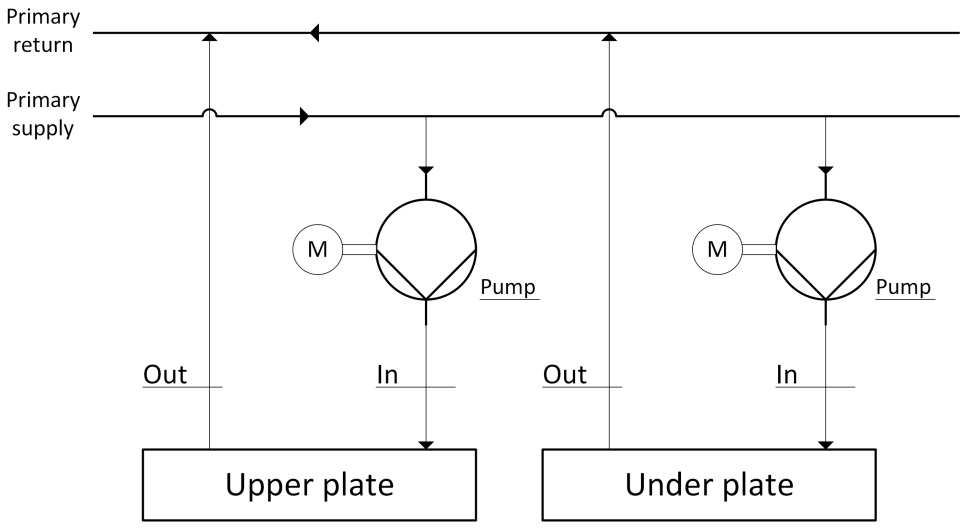

Figure 3.15 – Simplified schematic view of a coating press heating circuit

The total thermal energy consumption rate of the press BP_n will be given by the sum of the energy used in each circuit (Equation 3.13).

$$\dot{Q}_{BPn} = \dot{V}_{up_n}\rho_{to_{up}}C_{p_{to_{up}}}\Delta T_{up_n} + \dot{V}_{un_n}\rho_{to_{un}}C_{p_{to_{un}}}\Delta T_{un_n} \tag{3.13}$$

Where:

$\dot{q}_{p_n}$ = thermal energy rate usage by BP_n [kW]
$\dot{V}_{up_n}$ = upper circuit pumped thermal oil volumetric flow rate of BP_n [m^3/s]
$\rho_{to_{up}}$ = thermal oil density at average temperature of BP_n upper circuit [kg/m^3]
$C_{p_{to_{up}}}$ = specific heat of the thermal oil at average temperature of BP_n upper circuit [kJ/(kg·K)]
ΔT_{up_n} = thermal oil temperature difference of BP_n upper circuit [K]
$\dot{V}_{un_n}$ = upper circuit pumped thermal oil volumetric flow rate of BP_n [m^3/s]
$\rho_{to_{un}}$ = thermal oil density at average temperature of BP_n under circuit [kg/m^3]
$C_{p_{to_{un}}}$ = specific heat of the thermal oil at average temperature of BP_n under circuit [kJ/(kg·K)]
ΔT_{un_n} = thermal oil temperature difference of BP_n under circuit [K].

BP9 press features two heating circuits for each plate, the main heating circuit with a higher thermal oil flow rate and the other with a lower flow rate in counter current. Thus, for the thermal energy balance of this press, will be added the respective flow rates and temperature differences of each counter current circuit to Equation 3.13.

Chapter 4

THERMAL ENERGY BALANCE

In this chapter, will be applied the energy balance model depicted in the previous section with the average collected values of the operation in 2023. The monthly evolution of that year will be later presented in Chapter 5.

4.1 Thermal energy plant balance

In this section, will be applied the energy balance to the control volume depicted in Figure 3.11 of Chapter 3.

The energy output from biomass can be quantified by considering the mass of biomass that was consumed and its LHV. The product of the last two results in the amount of energy produced in a given period of time, such as a year. To determine the energy rate, the total mass of biomass can be converted to an average mass flow rate by dividing it by the working hours of the thermal energy plant and then by multiplying with the corresponding LHV, according to the first term of Equation 3.4. Table 4.1 showcases these calculations for the year 2023, considering the different types of fuel consumed, the corresponding LHV presented in Table 3.2 and the working hours of the thermal energy plant in that year. Wood, as biomass and as raw material for the process, undergoes moisture analysis upon arrival at the plant. This analysis determines the dry basis mass, from which all subsequent mass calculations are done. Thus, the biomass burned in the boiler is presented on a dry basis.

Table 4.1 – Biomass energy balance

Biomass type	**Mass** [t]	**LHV** [MJ/kg]	**Energy** [MWh]	**Power** [MW]	**Working time** [h]
Recycled wood chips db	16 531.0	17.67	81 159.3	9.690	-
Bark db	2 679.00	18.73	15 499.1	1.850	-
Fines db	472.458	15.60	2 047.32	0.244	-
Chopped forest biomass db	297.369	17.10	1 412.51	0.169	-
Black dust db	12 389.7	17.55	60 400.0	7.211	-
White dust db	4 583.01	18.10	23 042.3	2.751	-
Total	**41 822.8**	**-**	**183 561**	**21.92**	**8376**

Thus, the first term of Equation 3.4 results in the following:

$$\dot{m}_1 LHV = 21.92 \quad MW \tag{4.1}$$

Dividing the total mass of biomass burned in the boiler in 2023 (41 821.83 t) by the working hours results in a flow rate of 4.45 t/h out of the specified maximum of 28.50 t/h, which represents 16 % of the maximum fuel flow rate capacity. The power output from fuel of 21.92 MW represents 48 % of the load factor, out of the 45.7 MW specified maximum power. Furthermore, the biomass consumption in 2023 corresponded to 15 783.37 toe.

The thermal energy plant features flow meters in the primary, secondary air but does not feature an oxygen probe in the combustion room, neither flow meters in the tertiary air intake, air intake of the mixing chamber and the hot gas exit to the driers. Thus, it is not possible to quantify the efficiency of the combustion and a complete thermal energy balance of the thermal energy plant. The hot gas flow from the thermal energy plant will be later estimated in the dryer's energy balance.

For the thermal oil heat exchanger energy balance the average thermal oil input and output recorded temperatures in 2023 were used and the values are presented in Table 4.2.

Table 4.2 – Thermal oil temperatures in heat exchanger

	TO in	TO out
Temperature [ºC]	247.8	256.2

When in operation, the thermal oil flow in the heat exchanger and the flue gas flow fluctuate as a function of the demand. As the most energy demanding consumer is the continuous line press, this equipment indirectly dictates these flows. The average recorded thermal oil flow in the heat exchanger is of 590 m^3/h. Thermal oil density can be calculated using Equation 3.1 at the average temperature from Table 4.2, which results in:

$$\begin{aligned} &\rho = 879.41 + 0.5992 \cdot T && [kg/m^3] \\ &\Rightarrow \rho = 879.41 + 0.5992 \times 252 && [kg/m^3] \\ &\Rightarrow \rho = 1030.41 && [kg/m^3] \end{aligned} \tag{4.2}$$

The thermal oil specific heat is calculated according to Equation 3.2 such that:

$$\begin{aligned} &C_{p_{to}} = \frac{4.187}{\sqrt{\rho/1000}}(0.403 + 0.00081 \cdot T) && [kJ/(kg \cdot K)] \\ &\Rightarrow C_{p_{to}} = \frac{4.187}{\sqrt{1030.41/1000}}(0.403 + 0.00081 \cdot 252) && [kJ/(kg \cdot K)] \\ &\Rightarrow C_{p_{to}} = 2.504 && [kJ/(kg \cdot K)] \end{aligned} \tag{4.3}$$

The power received by the thermal oil in the heat exchanger is calculated by Equation 3.5 and the resulting energy is obtained by multiplying the power by the operating hours. This parameters are presented in Table 4.3.

Table 4.3 – Thermal oil heat exchanger energy balance

$\dot{q}_{to}$ [MW]	Working time [h]	q_{to} [MWh]
3.61	8 376	30 273.84

4.2 Hot gas users energy balance

As the plant does not feature any air intake flow meters in the mixing chamber nor in the intermediate flows of the dryers control volume, it is not possible to quantify the actual mass flow of hot gases (Points 9, 10, 12, 13, 14 and 16 of Figures 3.11 and 3.13). However, since it is expected that a high fraction of hot gas is air from air mixing intakes (points 6, 9 and 13) and it has a high concentration of Nitrogen from the excess air combustion of biomass, one can treat this flow as being 100 % hot atmospheric air and the flow can be quantified by the volumetric flow rate of the fans situated in Points 11 and 15 of Figure 3.13. For the volumetric flow rate, it will be considered that it varies linearly as a function of the fan speed load, which is monitored by internal software. Thus, for each fan, the nominal volumetric flow rate corresponds to a fan speed load of 100 %.

4.2.1 Recalor

For the energy balance using Equation 3.8 the following simplification will be made:

$$\dot{q}_{Rec} = \dot{m}_{13} C_p (T_{12} - T_{13}) \tag{4.4}$$

The specific heat (C_p) of air is calculated by *EES - Engineering Equation Solver* software at the average temperature of T_{12} and T_{13} and the mass flow rate $\dot{m}_{13}$ is given by the following equation:

$$\dot{m}_{13} = \dot{V}_{13} \rho_{13} load \tag{4.5}$$

where:

$\dot{V}_{13}$ = Recalor fan nominal volumetric flow rate [m^3/h]
ρ_{13} = Hot gas density at the outlet temperature calculated by *EES* [kg/m^3]
$load$ = Load of the fan motor [%].

These parameters and the calculation result of the mass balance are presented in Table 4.4.

Table 4.4 – Recalor hot gas mass flow rate parameters

$\dot{V}_{13}$ [m^3/h]	ρ_{13} [kg/m^3]	$load$ [%]	$\dot{m}_{13}$ [kg/h]
185 000	0.9349	98.24	169 918.18

The outlet T_{13} and intlet T_{12} temperatures are recorded by the internal monitoring software. The required parameters, including the C_p result given by *EES* and the solution of Equation 4.4 are presented in Table 4.5.

Table 4.5 – Recalor thermal energy balance

$\dot{m}_{13}$ [kg/h]	C_p [kJ/(kg·K)]	T_{13} [°C]	T_{12} [°C]	$\dot{q}_{Rec}$ [MW]	Working time [h]	q_{Rec} [MWh]
169 918.18	1.017	98.59	278.72	8.7	6 675	59 047.7

Equation 3.10 quantifies the useful energy rate to evaporate water from wood particles. The necessary parameters for the equation and the energy rate result are shown in Table 4.6. An internal monitoring software measures and records the mass flow rate of wood, initial temperature and moisture content of wood particles and their final moisture content. The considered values for these parameters are the calculated average during operation in 2023. The total operating hours in 2023 are multiplied by the energy rate to determine the useful energy used in drying wood particles.

Table 4.6 – Recalor water evaporation energy balance

$\dot{m}_{wood}$	[kg/h]	23 488.2
C_{p_w}	[kJ/(kg·K)]	1.871
T_{evap}	[°C]	100
T_{w_i}	[°C]	22
λ	[kJ/kg]	2 257
W_i	[%]	31.15
W_f	[%]	2.23
$\dot{q}_{dry_{Rec}}$	[MW]	4.64
Working time	[h]	6 675
$q_{dry_{Rec}}$	[MWh]	33 683.13

One can calculate the efficiency of the drying process of Recalor ($\eta_{dry_{Rec}}$) by $\eta_{dry} = q_{dry_{Rec}}/q_{Rec}$, which results in an average efficiency of 50.3 % in 2023, with a peak efficiency of 71.5 % in January (Appendix A).

4.2.2 BSH

The energy balance method for BSH will be the same as the one used in Recalor. The required parameters and the mass balance result are shown in Table 4.7.

Table 4.7 – BSH hot gas mass flow rate parameters

$\dot{V}_{17}$ [m^3/h]	ρ_{17} [kg/m^3]	*load* [%]	$\dot{m}_{17}$ [kg/h]
214 200	0.9236	66.4	131 380.8

The required parameters and the energy balance result are shown in Table 4.8.

Table 4.8 – BSH thermal energy balance

$\dot{m}_{17}$ [kg/h]	C_p [kJ/(kg·K)]	T_{17}] [°C]	T_{16}[°C]	$\dot{q}_{BSH}$ [°C]	Working time [h]	q_{BSH} [MWh]
131 380.8	1.018	100	342.9	9.0	6 781	61 554.9

The required parameters and the water evaporation energy balance are shown in Table 4.9.

Table 4.9 – BSH water evaporation energy balance

$\dot{m}_{wood}$	[kg/h]	15 100.96
C_{p_w}	[kJ/(kg·K)]	1.871
T_{evap}	[°C]	100
T_{w_i}	[°C]	22
λ	[kJ/kg]	2 257
W_i	[%]	29.76
W_f	[%]	1.79
$\dot{q}_{dry_w}$	[MW]	2.9
Working time	[h]	6 736
q_{dry_w}	[MWh]	21 374.5

These energy balances result in an average efficiency of the drying process of BSH, $\eta_{dry_{BSH}} = 60.6\%$, with a peak efficiency of 76.0 % in January (Appendix A).

4.3 Thermal oil users energy balance

According to Section 3.5.3, each thermal oil consumer has several heating circuits that are fitted with a pump working at a certain load, which results in a flow rate according to the pump characteristic curve. The inlet and outlet temperatures were recorded with the temperature gauges fitted at the respective supply and return circuits.

4.3.1 Continuous line press

To quantify the thermal oil volumetric flow rate in each heating circuit were used measurements done with a portable power meter at a given period of time of each ESV drive motor (Figures 4.1, 4.2, 4.3, 4.4 and 4.5) and the respective average power results were used. To convert drive motor power into pump power on the axle it was considered the efficiency of the pump and drive motor group given by:

$$Efficiency = \frac{Axle\ pump\ power}{Drive\ power} \quad [\%] \tag{4.6}$$

Which results in:

$$\frac{Axle\ pump\ power}{Drive\ power} = \frac{Calculated\ axle\ pump\ power}{Measured\ drive\ power} \tag{4.7}$$

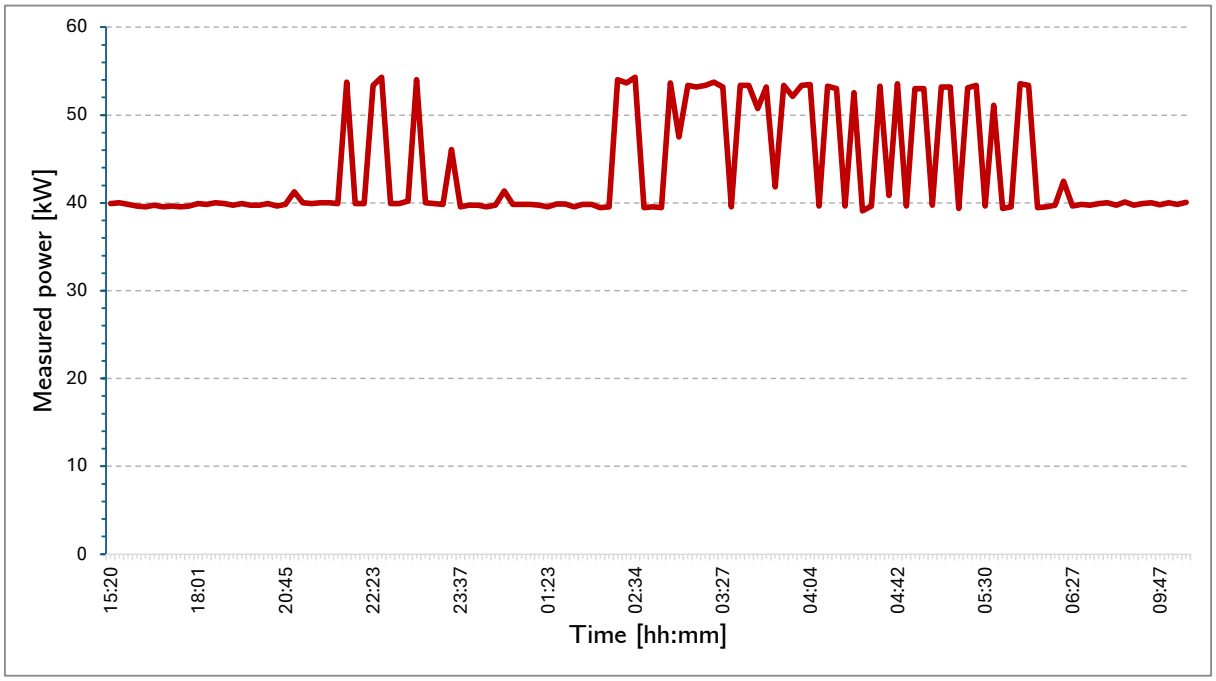

Figure 4.1 – Pump 1 drive motor load chart.

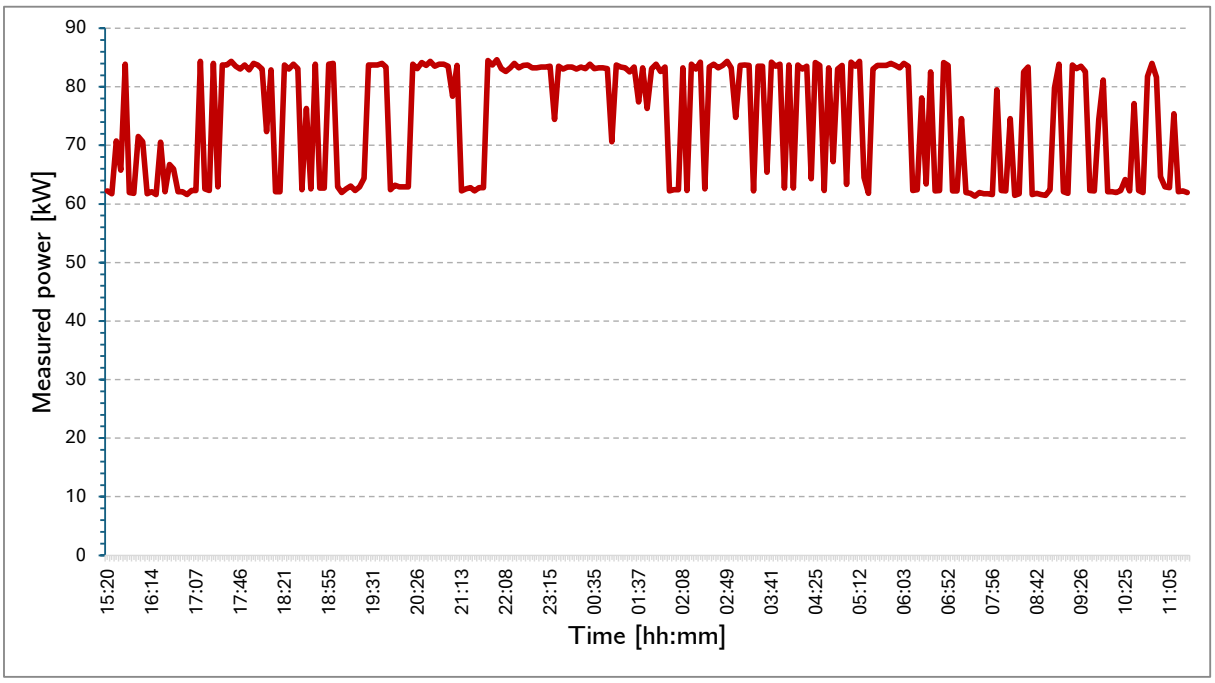

Figure 4.2 – Pump 2 drive motor load chart.

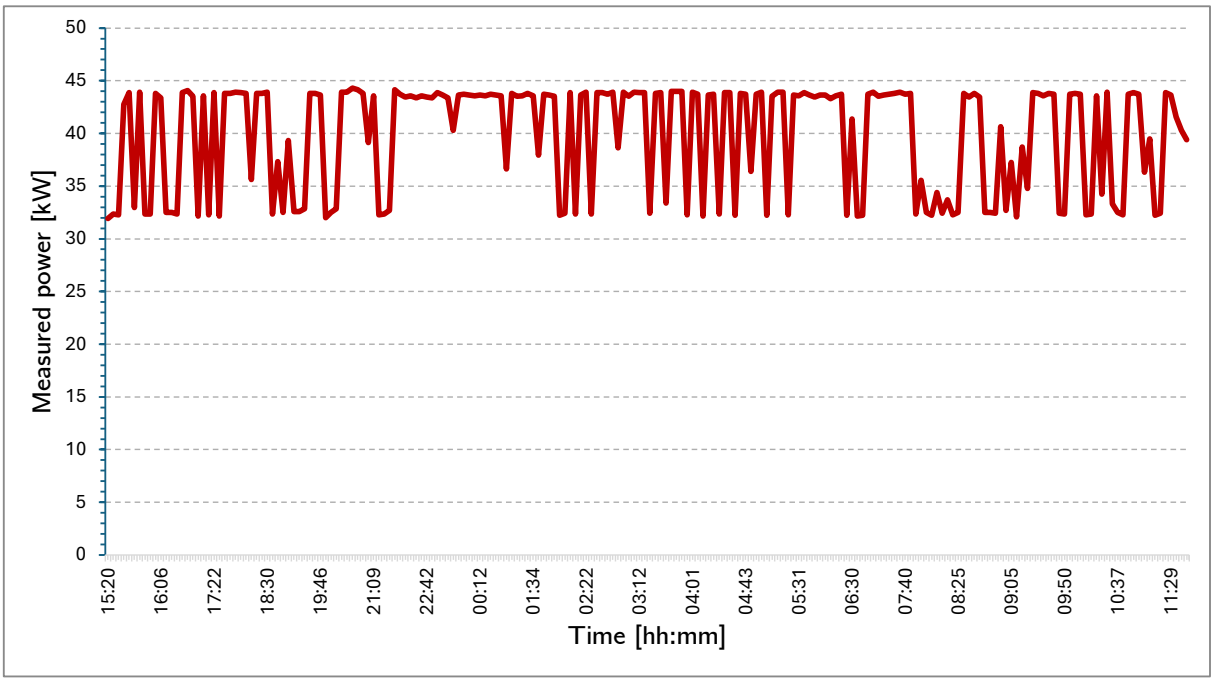

Figure 4.3 – Pump 3 drive motor load chart.

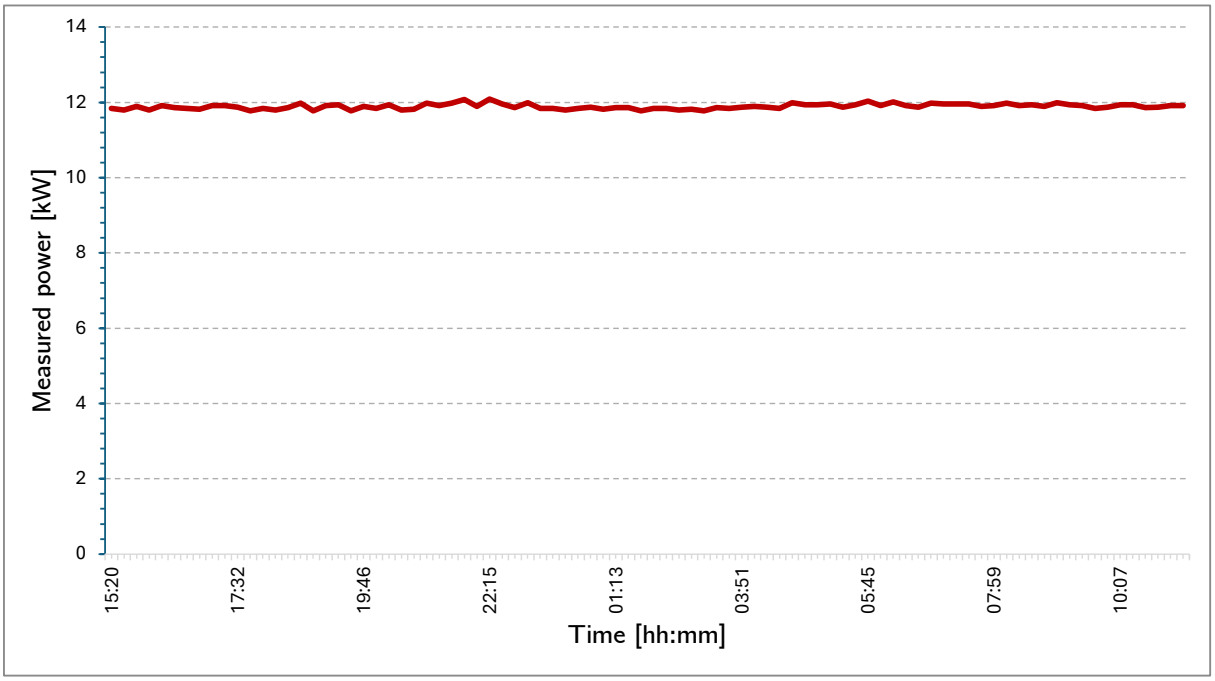

Figure 4.4 – Pump 4 drive motor load chart.

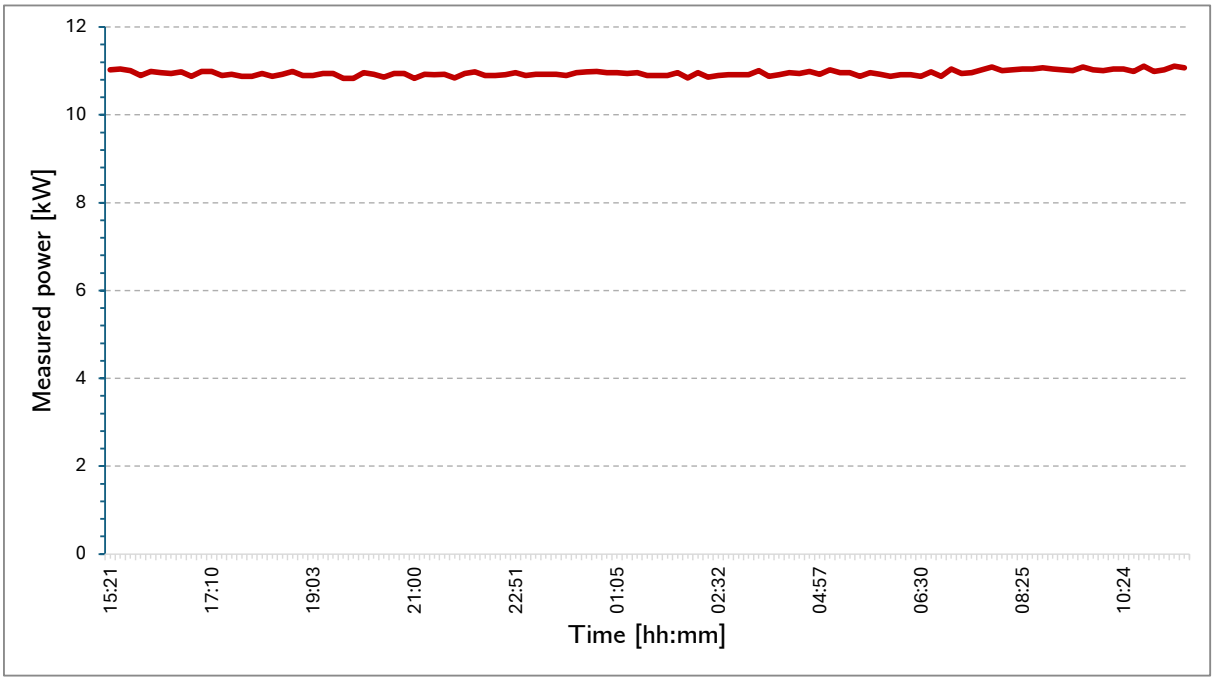

Figure 4.5 – Pump 5 drive motor load chart.

The specified, measured and calculated pump and drive motor parameters are shown in Table 4.10.

Table 4.10 – Continuous line press heating circuit pumps and drive motors specifications

Circuit	Circuit 1	Circuit 2	Circuit 3	Circuit 4	Circuit 5
Pump	NTT 125/400	NTT 200/400	NTT 150-400	NTT 125/250	NTT 125/250
Diameter [mm]	420	420	374	264	264
Pump power [kW]	54.3	85.9	45	12.4	12.4
Drive power [kW]	55	90	55	15	15
Efficiency [%]	98.7	95.4	81.8	82.7	82.7
Measured drive power [kW]	41.63	74.31	40.28	11.87	10.93
Calculated pump power [kW]	41.10	70.92	32.96	9.81	9.04

To calculate the volumetric flow rate from the calculated axle pump power it was assumed a linear evolution from each pump curve (Appendix B), such that:

$$\dot{V}_1 = \frac{(P_2 - 15) \cdot 330}{(52.71 - 15)} \tag{4.8}$$

$$\dot{V}_2 = load \cdot 600 \tag{4.9}$$

$$\dot{V}_3 = \frac{(P_2 - 19) \cdot 382}{(52.55 - 19)} \tag{4.10}$$

$$\dot{V}_{4,\,5} = \frac{(P_2 - 4) \cdot 200}{(12.11 - 4)} \tag{4.11}$$

where:

$\dot{V}_n$ = Circuit n pump volumetric flow rate [m^3/h]
P_2 = Calculated axle pump power from Equation 4.7 [kW]
$load$ = Measured drive power or drive power from Table 4.10 [%].

The conversion from volumetric flow rate to mass flow rate is made using thermal oil density calculated from Equation 3.1 at the average temperature of the inlet and outlet of each heating circuit. These temperatures are recorded in real time and it was assumed that remained rather constant during the continuous line press normal operation. With the mass flow rate, temperature differences and working time of the press in 2023, it is possible to calculate the thermal energy and thermal energy usage of the continuous line press in 2023 (Table 4.11).

Table 4.11 – Continuous line press thermal energy balance

Circuit	$\dot{V}$ [m^3/h]	$\dot{m}$ [kg/h]	T_{in} [ºC]	T_{out} [ºC]	$\dot{q}$ [MW]	Working time [h]	q [MWh]
Circuit 1	228.40	233 562	247.6	230.3	2.77	6 106.2	16 928
Circuit 2	495.4	507 051	243.2	237.8	1.88	6 106.2	11 490
Circuit 3	207.3	211 873	239.7	236.9	0.41	6 106.2	2 483.7
Circuit 4	143.34	143 774	203.3	201.1	0.21	6 106.2	1 269.7
Circuit 5	124.18	123 774	196.4	195.2	0.10	6 106.2	593.36
Total					**5.37**		**32 765**

4.3.2 Impregnation lines

Equation 3.12 will be used to quantify the thermal energy rate for each impregnation line.

4.3.2.1 VITS1

For each heating circuit of VITS1, it was considered an average drive motor load of 75 % during operation. The volumetric flow rate was estimated using the drive motor and pump group efficiency and the pump curve (Appendix B), similar to Section 4.3.1 procedure. The used parameters for each heating circuit are shown in Table 4.12.

Table 4.12 – VITS1 pumps and drive motors specifications

Circuit	Drive power [kW]	Pump power on axle [kW]	Efficiency [%]	Drive load [%]	Calculated pump power on axle [kW]	$\dot{V}$ [m^3/h]
Circuit 1	5.5	3.67	66.7	75	2.75	17.83
Circuit 2	5.5	3.67	66.7	75	2.75	17.83
Circuit 3	5.5	3.67	66.7	75	2.75	17.83
Circuit 4	5.5	3.67	66.7	75	2.75	17.83
Circuit 5	6.3	3.67	66.7	75	2.75	17.83

To calculate the thermal energy rate, the thermal oil inlet and outlet temperatures of each heating circuit were registered from the available temperature gauges and assuming that the temperatures remain constant during operation. The fluid material properties were calculated from Equations 3.1 and 3.2. The thermal energy usage of the continuous line press in 2023 was calculated considering the line working hours in that year. This information, the calculated thermal power and thermal energy usage are shown in Table 4.13.

Table 4.13 – VITS1 thermal energy balance

Circuit	$\dot{m}$ [kg/h]	T_{in} [ºC]	T_{out} [ºC]	$\dot{q}$ [MW]	Working time [h]	q [MWh]
Circuit 1	16 107.68	147.5	142	0.06	2781	
Circuit 2	16 107.68	162.5	155	0.08	2781	212.66
Circuit 3	16 107.68	159	154	0.05	2781	141.78
Circuit 4	16 107.68	149	141	0.08	2781	226.84
Circuit 5	16 107.68	135	135	0.00	2781	0.00
Total				0.27		737.23

4.3.2.2 VITS2

For each heating circuit of VITS2 the calculation method is the same as for VITS1. The considered heating pumps and drive motors specifications are shown in Table 4.14 and the energy balance is shown in Table 4.15.

Table 4.14 – VITS2 pumps and drive motors specifications

Circuit	Drive power [kW]	Pump power on axle [kW]	Efficiency [%]	Drive load [%]	Calculated pump power on axle [kW]	$\dot{V}$ [m^3/h]
Circuit 1	7.5	3.67	48.9	75	2.75	17.83
Circuit 2	7.5	3.67	48.9	75	2.75	17.83
Circuit 3	7.5	3.67	48.9	75	2.75	17.83
Circuit 4	7.5	3.67	48.9	75	2.75	17.83
Circuit 5	7.5	3.67	48.9	75	2.75	17.83
Circuit 6	7.5	3.67	48.9	75	2.75	17.83

Table 4.15 – VITS2 thermal energy balance

Circuit	$\dot{m}$ [kg/h]	T_{in} [°C]	T_{out} [°C]	$\dot{q}$ [MW]	Working time [h]	q [MWh]
Circuit 1	17 221.3	145	144	0.01	6 798.37	63.61
Circuit 2	17 317.4	156	151	0.05	6 798.37	318.07
Circuit 3	17 253.4	149	146	0.03	6 798.37	190.84
Circuit 4	17 285.4	155	146	0.08	6 798.37	572.53
Circuit 5	16 932.9	120	115	0.05	6 798.37	318.07
Circuit 6	16 852.8	110	110	-	6 798.37	-
Total				0.24		1 653.62

4.3.3 Melamine coating lines

During the work, only the BP8 press was equipped with temperature sensors installed at the inlet and outlet of each heating circuit. In this press, the temperature sensors are digitally integrated into the internal process monitoring software, which allows real time and historical temperature tracking.

The flow rate of both heating circuits in BP8 press was determined through calculations based on the pumps and drive motors specifications (Appendix B), for which an expected average operating load of the ESV motor of 67.8 % was considered. Since the pump curve is unknown, electric power can be converted into volumetric flow rate assuming a linear evolution, where 100 % load would correspond to the nominal volumetric flow rate.

For the remaining presses, it was also estimated the volumetric flow rate based on pump curves and the average operating drive motor load.

The last obtained parameters are presented in Table 4.16.

Table 4.16 – Coating lines pumps and drive motors specifications

Line	Circuit		Pump	Drive power [kW]	Drive load [%]	$\dot{V}$ [m^3/h]
BP6	Upper		NTT80-160	11	75	46.50
	Under		NTT80-160	7.5	75	46.50
BP7	Upper		NTT80-200	22	75	122.25
	Under		NTT80-200	22	75	122.25
BP8	Upper		Etanorm SY80-200	30	67.7	131.95
	Under		Etanorm SY80-200	30	65.3	127.4
BP9	Upper	Main	NTT80-160	15	75	108.75
		Counter	NTT50-160	5.5	75	42.75
	Under	Main	NTT80-160	15	75	108.75
		Counter	NTT50-160	5.5	75	42.75

The thermal power and energy usage of each press was calculated according to Equation 3.13 with the average inlet and outlet temperatures of each heating circuit of BP8 in 2023. The calculated thermal power and thermal energy usage for each heating circuit of BP8 are shown in Table 4.17.

Table 4.17 – BP8 thermal energy balance

Line	Circuit	$\dot{m}$ [kg/h]	T_{in} [°C]	T_{out} [°C]	$\dot{q}$ [MW]	Working time [h]	q [MWh]
BP8	Upper	130 298.91	183.3	177.4	0.50	3 803.88	1 888.49
	Under	125 805.84	182.8	178.3	0.36	3 803.88	1 369.36
Total					0.86	3 803.88	3 256.52

As seen, a thermal energy usage calculation by temperature measurement of BP6, BP7 and BP9 was not possible due to missing instrumentation. The founded solution was the assumption that BP6, BP7 and BP9 work on average at each nominal thermal load (Table 3.5), resulting in the thermal balance of the melamine coating lines presented in Table 4.18.

Table 4.18 – Melamine coating lines energy balance

Line	$\dot{q}$ [MW]	Working time [h]	q [MWh]
BP6	0.255	2 256.01	575.28
BP7	0.640	3 972.24	2 542.23
BP8	0.856	3 803.88	3 256.52
BP9	0.698	4 595.68	3 206.87

Chapter 5

RESULTS, DISCUSSION AND IMPROVEMENT PROPOSALS

5.1 Results

The thermal energy balance of the Oliveira do Hospital plant was based on the consumed biomass, its LHV, the estimated flows and measured temperatures of hot gas and thermal oil.

Figure 5.1 shows the monthly evolution of the thermal energy balance with data from Appendix A. The chart suggests that biomass consumption in MWh, which results in thermal energy generated at the energy plant, is strongly related to thermal energy consumption by the users, with the dryers being the most energy demanding, followed by the continuous line press, melamine coating (MFC), and ending with the impregnation lines.

Additionally, the evolution of production volume and working hours, available in Appendix B, aligns with the thermal energy consumption trend, notably showing a lower spike in August, the month designated for the annual maintenance shutdown.

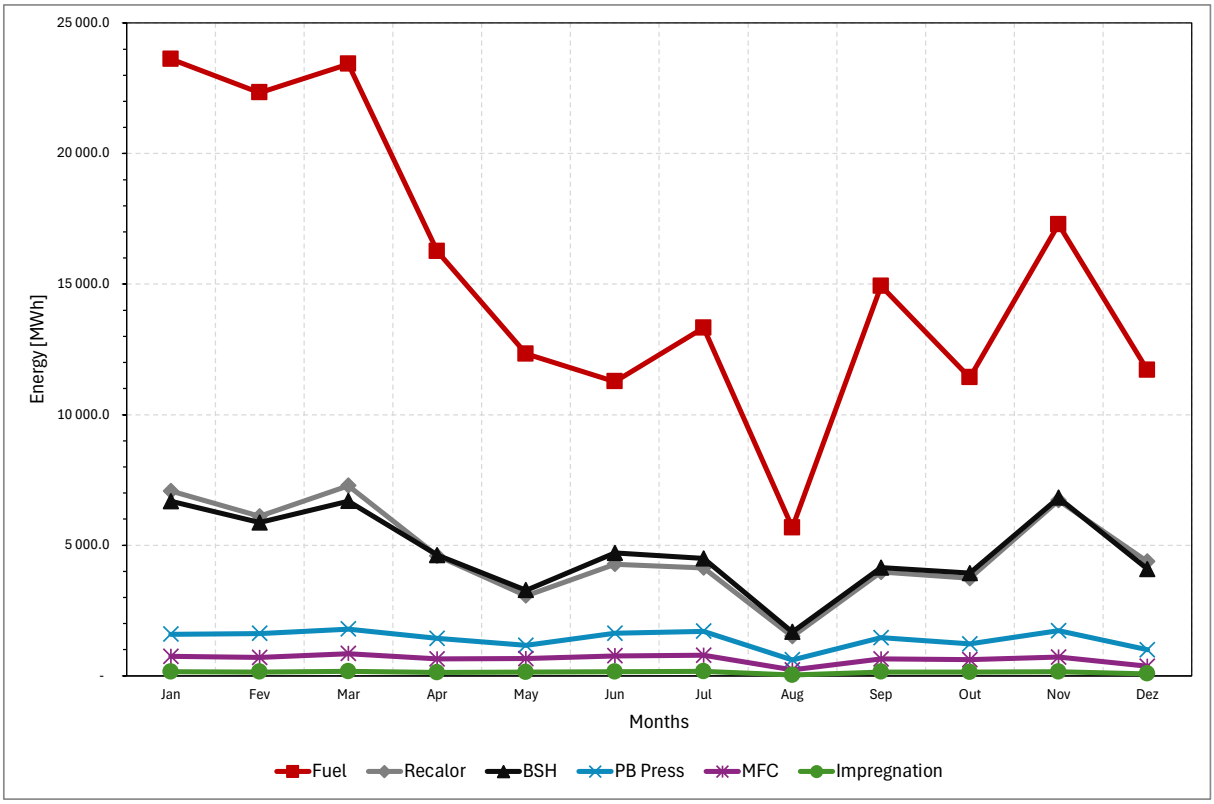

Figure 5.1 – Thermal energy balance monthly evolution.

Additionally to the conducted analysis, the energy balance of the energy plant control volume presented in 4 was estimated. The plant does not feature air flow meters in the tertiary air intake of the combustion room and flow meters in the mixing air intakes. Thus, it was not possible to estimate a complete combustion and thermal energy plant energy balance.

Table 5.1 shows the energy balance of the hot gas based on the mass flow of fuel, its LHV, the mass flow and temperature of hot air entering the combustion room (primary and secondary air), the heat lost in the thermal oil heat exchanger, the mass flow and temperature of hot gas entering the dryers, and the remaining mass flow of air that enters the system is calculated such that the mass balance of the system is completed:

$$\dot{m}_4 + \dot{m}_8 + \dot{m}_{11} + \dot{m}_{15} = \dot{m}_{12} + \dot{m}_{16} - \dot{m}_1 - \dot{m}_2 - \dot{m}_3 \tag{5.1}$$

Table 5.1 – Hot gas thermal energy balance

Flow direction	Control point	Description	$\dot{m}$ [t/h]	T [°C]	h [kJ/kg]	LHV [MJ/kg]	$\dot{q}$ [MW]
In	1	Fuel	4.45	-	-	17.74	21.92
	2	Primary air	30.11	14.68	288.20	-	2.41
	3	Secondary air	36.76	14.68	288.20	-	2.94
	4, 8, 11 and 15	Tertiary air and other air intakes	231.08	14.68	288.20	-	18.50
Out	12 and 16	Dryers intake	302.4	309.03	588.7	-	49.45
	$5 \rightarrow 6$	Heat lost to thermal oil	-	-	-	-	3.61

The integrity of information on fuel flow, which relies on calculations rather than mass measurements in the case of white dust, and the LHV value precision, considering that the last fuel analysis was conducted in 2016, may influence the accuracy of the presented hot gas thermal energy balance results.

5.1.1 Relevant variables

The monthly balance analysis (Appendix A), which includes the energy balance based on the developed model and relevant variables for both the energy plant and thermal energy consumers, unveils the correlation between different parameters (Table 5.2).

Table 5.2 – Relevant variables

Parameter	**Relevant variable**	**Chart**
Dryer thermal energy usage [MWh]	Dried particles [t]	5.2 and 5.4
Dryer thermal power [MW]	Particles moisture content [%]	5.3 and 5.5
Continuous line press thermal energy usage [MWh]	PB production [m^3]	5.6
BP8 line thermal energy usage [MWh]	BP8 production [m^3]	5.7
Melamine coating lines thermal energy usage [MWh]	Melamine production [m^3]	5.8
Impregnation lines thermal energy usage [MWh]	Impregnation production [m^2]	5.9

The charts (Figure 5.2 to 5.9) illustrate this correlation, and the R^2 value, when close to 1, is an indicator of a high correlation.

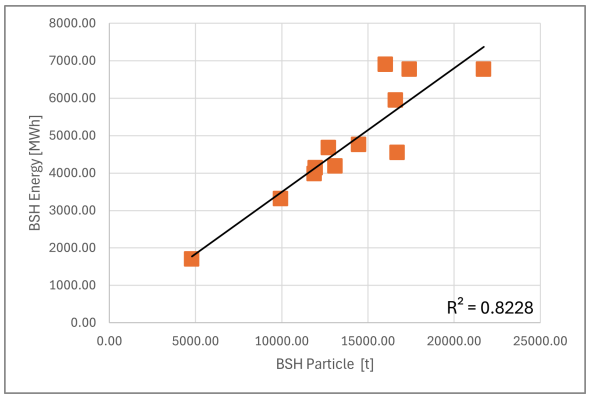

Figure 5.2 – BSH energy [MWh] vs Dried particles [t].

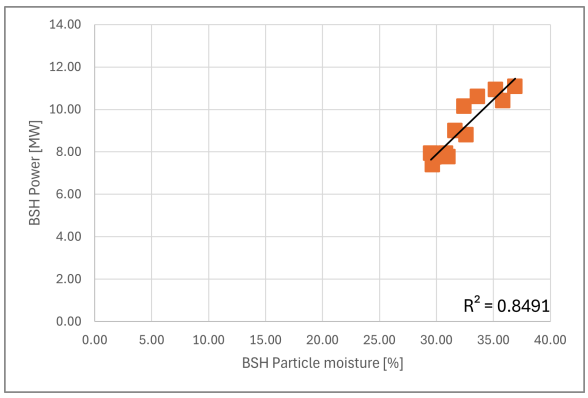

Figure 5.3 – BSH power [MW] vs Particle moisture [%].

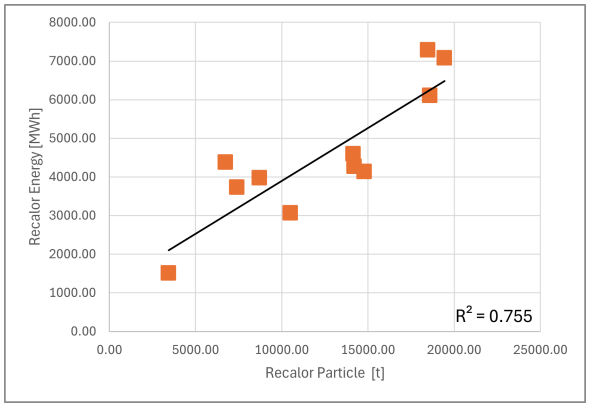

Figure 5.4 – Recalor energy [MWh] vs Dried particles [t].

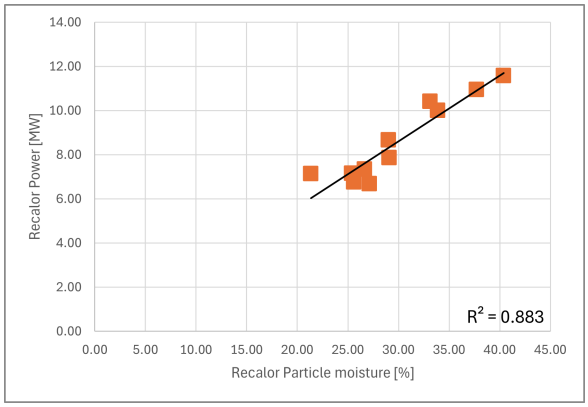

Figure 5.5 – Recalor power [MW] vs Particle moisture [%].

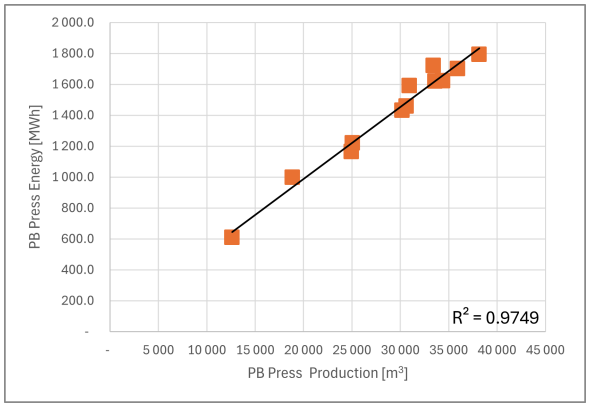

Figure 5.6 – Continuous line press energy [MWh] vs production [m^3].

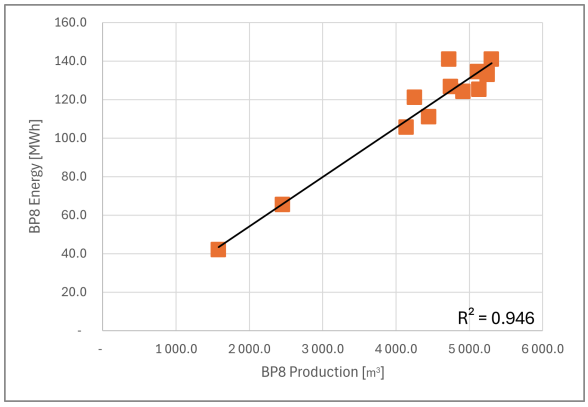

Figure 5.7 – BP8 line energy [MWh] vs production [m^3].

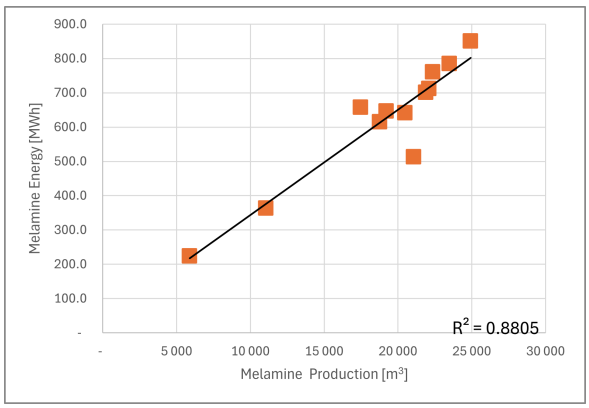

Figure 5.8 – Melamine lines energy [MWh] vs production [m^3].

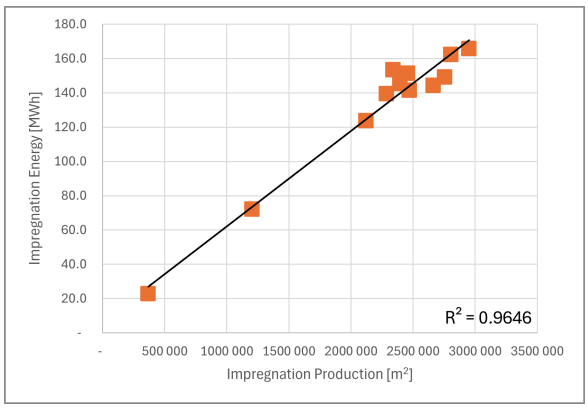

Figure 5.9 – Impregnation lines energy [MWh] vs production [m^2].

Particle flow and particle moisture were the two identified variables for the dryers. The R^2 value ranging between 0.76 and 0.88 revealed that both variables influence the energy consumption BSH and Recalor dryers, with one outlier disregarded in the Recalor analysis. For both dryers, particle moisture has a more pronounced impact on thermal energy consumption.

The analysis of thermal oil energy consumption suggests a strong correlation between energy consumption and production volume (m^3 or m^2), with an R^2 value consistently higher than 0.9. However, in the context of this research, the thermal oil flow rate and temperatures remained constant in the considered year, leaving working time as the only variable parameter influencing the energy balance results, except for BP8 where thermal oil temperature monitoring was available. This implies that for those users the strong correlation that was found between energy consumption and production volume is actually a reflection of the relationship between production volume and working hours.

5.2 Improvement proposals

In this subsection, it will be suggested improvements to address the identified constraints during the on-site research. These includes solutions found in literature aiming to improve the accuracy of the thermal energy balance model results and improving thermal energy efficiency.

5.2.1 Measurement and control

Lack of measurement and control of parameters in the several stages of the thermal energy flow in the plant was the main difficulty encountered during the research. The founded workaround was to estimate values based on the most reliable measurement, information or assumption, which may result in inaccuracies in some of the developed energy balance model results.

The air/fuel ratio settings in the energy plant depend on the biomass quality, which includes factors such as its LHV, moisture content, and ash composition. Thus, conducting a new fuel analysis would yield updated results and allow for an evaluation of the existing air mixing parameters.

As depicted in the research, the O_2 concentration probe inside the combustion room is the most straightforward tool to assess the air/fuel mixture and combustion efficiency. A new oxygen level probe would result in a better assessment of the combustion.

Flue and hot gas energy flows might be quantified with proper measurement. In this research, mass flow rate and enthalpies were computed considering a composition of 100 % air and the volumetric flow rate was estimated from the dryers fan specifications. Flue and hot gas energy can be calculated with more precision with the following measurements:

1. Gas chemical composition (components and respective fractions) that can be measured using electrochemical or infrared probes, along temperature and pressure sensors to calculate the actual fluid density (ρ) and specific heat (C_p);

2. Volumetric flow rate with cross section area information and the most reliable velocity measurement technology for the application (*e.g.* pitot tube or ultrasound).

For the hot gas, the assessment can be done by measuring the flow of atmospheric air that mixes with the flue gas, excluding the need for chemical composition measurement. In either case, this instrumentation requires to verify some conditions outlined in EN 16911-2 norm (*e.g.* installation in a fully developed region of the flow - distanced 25 D_h upstream and 5 D_h downstream, that may vary depending on the type of elements in the ducts).

The thermal oil energy balance can be calculated with more precision using the following measurements:

1. Volumetric flow rate meter either downstream or upstream of the thermal oil heat exchanger, where temperature sensors are already in place, to calculate the heat transferred to thermal oil (Equation 3.5);

2. Volumetric flow rate meter in each thermal heating circuit of the users (specifically those with pumps);

3. Temperature sensors at the inlet and outlet of each heating circuits where they are currently missing.

These measurement proposals, along with the developed biomass mass flow balance model, require a monitoring, recording, and trend control software system to establish trends and analyze consumption patterns throughout the year, which allows improved control responses for the energy demand, increase in efficiency and advanced plant energy management system.

5.2.2 Plant maintenance

The measurement devices can become dirty, blocked and their electronic components can degrade leading to inaccurate readings over time. To mitigate these issues, regular maintenance including cleaning, verifying and recalibrating is necessary. This ensures equipment longevity and reliability of the instrumentation, which is crucial for the accuracy of the developed thermal balance model results.

This research has established that an important amount of ash is present in biomass and flue gas. Ash deposits in the heat exchanger surfaces form a layer of insulation, which has a negative impact in the heat transfer efficiency from the flue gas to thermal oil. Preventive inspection of the heat exchanger tubes may mitigate this effect.

5.2.3 Process engineering

As seen in Chapter 2, moisture in biomass negatively impacts its LHV, therefore reducing combustion efficiency. However, large-scale biomass drying is an energy-intensive technology, requiring significant amounts of both electric and thermal energy, with BSH and Recalor dryers being the most thermal energy-demanding users at the plant. Cost-effective drying methods, such as storing biomass during the hot dry season or using heated air from solar radiation (Figure 5.10) or waste heat from the existing dryers (BSH and Recalor) are options that may be worth further investigation, as drying biomass from a moisture content of 50 % to 30 % has a potential of thermal efficiency increase of 8.7 % (van Loo and Koppejan, 2008).

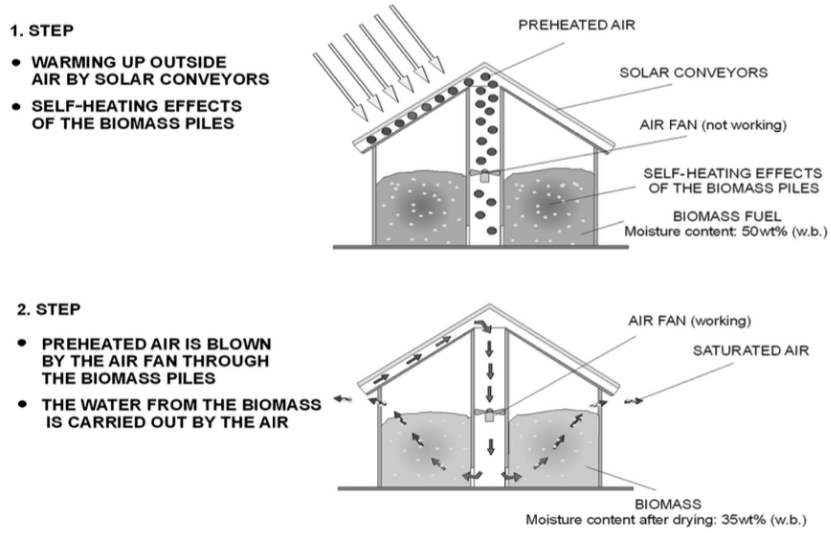

Figure 5.10 – Biomass drying with solar energy (van Loo and Koppejan, 2008).

Chapter 6

CONCLUSIONS AND FUTURE WORK PROPOSALS

This research was carried out with the aim of identifying and quantifying fuel consumption and thermal energy consumption, based on an energy balance model with possible improvement proposals.

The developed thermal energy balance model began with mapping the installation's thermal energy flows, followed by the monitoring and recording of the relevant variables. These included the consumption of biomass from external suppliers and wood rejects, as well as hot gas and thermal oil measurements of flow rates and temperatures at several key points in the energy flows.

The results of the developed thermal energy balance model revealed that thermal energy derived from biomass accounted for 183 561 MWh in 2023 which resulted in 61 % (*toe*) of the total energy consumption of the plant in that year, with the remainder being electricity and diesel. This substantial dependence on biomass highlights the importance of accurate thermal energy flow mapping for effective energy management.

As expected, the analysis of biomass consumption revealed a strong correlation with production patterns. Notably, BSH and Recalor dryers were identified as the major thermal energy consumers, for which extensive monitoring data was available, thus improving the result's accuracy. Thermal oil energy users' calculations were derived from the measurements of the required parameters, supplemented by assumptions and for some lines based on the specified thermal power by the supplier.

Correlations between energy consumption and production variables were established, indicating a clear influence of wet particles on dryers and production volume (m^3 or m^2) on thermal oil energy users. These findings highlight the importance of integrating production processes into energy management strategies to optimize and balance the efficiency of energy consumption and production.

The obtained thermal energy balance results were only possible due to the vast data and instrumentation available for the fuel and thermal energy flux. However, the lack of measurements and historical data recording of some flow parameters impacted the accuracy of the thermal energy balance model results. This highlights the need for improved instrumentation and data recording systems for reliable energy consumption tracking, management and continuous improvement. To address these concerns, proposals that require further investigation include the installation of instrumentation as well as biomass quality monitoring, focusing on moisture content, ash and LHV, proper maintenance of critical energy monitoring instruments and biomass quality improvement methods.

REFERENCES

Amamoto, M., Takahata, M., Fuji, T., and Kumagai, T. (2019). Efforts toward steam power plant utilized pulverized biomass exclusive firing technology, mitshubishi heavy industries technical review vol. 56 no. 3. Technical report.

Barma, M., Saidur, R., Rahman, S., Allouhi, A., Akash, B., and Sait, S. M. (2017). A review on boilers energy use, energy savings, and emissions reductions. *Renewable and Sustainable Energy Reviews*, 79:970–983.

Basu, P. (2018). *Biomass Gasification, Pyrolysis and Torrefaction*. Academic Press.

CIPEC (2009). *Energy savings toolbox: an energy audit manual and tool.* Canadian Industry Program for Energy Conservation.

Crawford, M. (2012). The american society of mechanical engineers - fluidized-bed combustors for biomass boilers. Accessed on March 2, 2024.

de Pinho, C. M. C. T. (2016). *Sistemas Térmicos*. Departamento de Engenharia Mecânica.

Gregg, J. S. and Smith, S. J. (2010). Global and regional potential for bioenergy from agricultural and forestry residue biomass. *Mitigation and Adaptation Strategies for Global Change*, 15:241–262.

Klass, D. L. (1998). *Biomass for renewable energy, fuels, and chemicals*. Academic Press.

Marshall Brain, Y. S. (2023). Howstuffworks: Boilers - how steam engines work. Accessed on March 1, 2024.

Mateos, E. (2019). Study on the potential of forest biomass residues for bio-energy. *The 2nd International Research Conference on Sustainable Energy, Engineering, Materials and Environment*.

Monteiro, E., Mantha, V., and Rouboa, A. (2012). Portuguese pellets market: Analysis of the production and utilization constrains. *Energy Policy*, 42:129–135.

Nhuchhen, D. and Afzal, M. (2017). Hhv predicting correlations for torrefied biomass using proximate and ultimate analyses. *Bioengineering*, 4:7.

Niemz, P., Teischinger, A., and Sandberg, D. (2023). *Springer Handbook of Wood Science and Technology*. Springer.

of Strathclyde, U. (2008). Biomass installation feasibility tool. Accessed on March 1, 2024.

of Texas, U. (2015). Chemistry 301: Bomb calorimetry. Accessed on March 1, 2024.

ORANG, N. and TRAN, H. (2015). Effect of feedstock moisture content on biomass boiler operation. *October 2015,TAPPI Journal*, 14:629–637.

Saidur, R., Abdelaziz, E., Demirbas, A., Hossain, M., and Mekhilef, S. (2011). A review on biomass as a fuel for boilers. *Renewable and Sustainable Energy Reviews*, 15:2262–2289.

Sheng, C. and Azevedo, J. (2005). Estimating the higher heating value of biomass fuels from basic analysis data. *Biomass and Bioenergy*, 28:499–507.

Skrifvars, B.-J., Laurén, T., Hupa, M., Korbee, R., and Ljung, P. (2004). Ash behaviour in a pulverized wood fired boiler—a case study. *Fuel*, 83:1371–1379.

van Loo, S. and Koppejan, J. (2008). *The Handbook of Biomass Combustion Co-firing*. Earthscan.

WBA (2022). Global bioenergy statistics 2022. Technical report, World Bioenergy Association.

Zhou, L.-P., Wang, B.-X., Peng, X.-F., Du, X.-Z., and Yang, Y.-P. (2010). On the specific heat capacity of cuo nanofluid. *Advances in Mechanical Engineering*, 2:172085.

Appendix A

MONTHLY ENERGY BALANCE

	Jan	Fev	Mar	Apr	May	Jun	Jul	Aug	Sep	Out	Nov	Dez	YTD
Working time [h]	744.0	672.0	744.0	720.0	744.0	720.0	744.0	360.0	720.0	744.0	720.0	744.0	**8 376.00**
Recycled wood chips [t db]	2 969.0	2 366.0	2 208.0	1 642.0	1 090.0	491.0	756.0	457.0	1 243.0	835.0	1 574.0	900.0	**16 531.00**
Recycled wood chips [MWh]	14 576.4	11 615.9	10 840.2	8 061.4	5 351.4	2 410.6	3 711.6	2 243.7	6 102.5	4 099.5	7 727.6	4 418.6	**81 159.34**
Bark [t db]	205.0	364.0	648.0	137.0	112.0	187.0	225.0	112.0	292.0	172.0	293.0	232.0	**2 979.00**
Bark [MWh}	1 066.6	1 893.8	3 371.4	712.8	582.7	972.9	1 170.6	582.7	1 519.2	894.9	1 524.4	1 207.0	**15 499.08**
Fines [t db]	70.8	83.7	87.3	52.6	-	25.3	-	-	47.4	-	25.6	79.8	**472.46**
Fines [MWh]	306.6	362.6	378.2	228.0	-	109.5	-	-	205.5	-	110.8	346.0	**2 047.32**
Chopped forest biomass [t db]	20.3	174.7	58.7	-	-	-	43.7	-	-	-	-	-	**297.37**
Chopped forest biomass [MWh]	96.6	829.7	278.8	-	-	-	207.4	-	-	-	-	-	**1 412.50**
White dust [t db]	376.4	369.8	430.5	425.9	446.0	394.0	430.5	134.4	377.3	411.9	354.6	431.8	**4 583.01**
White dust [MWh]	1 892.4	1 859.3	2 164.6	2 141.2	2 242.2	1 981.0	2 164.5	675.8	1 897.1	2 070.8	1 782.7	2 170.8	**23 042.34**
Black dust [t db]	1 164.7	1 184.9	1 311.5	1 047.7	851.8	1 187.9	1 245.3	445.2	1 067.7	893.3	1 259.9	730.0	**12 389.74**
Black dust [MWh]	5 678.0	5 776.2	6 393.6	5 107.3	4 152.6	5 790.9	6 070.8	2 170.3	5 205.1	4 354.7	6 142.0	3 558.6	**60 399.99**
Total Power [MW]	31.7	33.2	31.5	22.6	16.6	15.6	17.9	15.8	20.7	15.3	24.0	15.7	**21.92**
Total Energy [MWh]	23 616.6	22 337.5	23 426.9	16 250.8	12 328.8	11 265.0	13 324.9	5 672.5	14 929.4	11 419.8	17 287.5	11 701.0	**183 560.57**

Figure A.1 – Fuel energy balance per month - 2023.

	Jan	Fev	Mar	Apr	May	Jun	Jul	Aug	Sep	Out	Nov	Dez	YTD
Working time [h]	744.00	672.00	744.00	720.00	744.00	720.00	744.00	360.00	720.00	744.00	720.00	744.00	8 376.00
TO in temp [ºC]	252.49	254.94	252.18	251.05	254.57	251.59	249.34	213.58	242.92	255.02	250.59	245.34	247.80
TO out temp [ºC]	261.86	264.78	262.18	258.78	261.74	260.04	257.90	219.19	251.27	262.24	259.74	254.71	256.20
Density [kg/m3]	1 033.5	1 035.1	1 033.5	1 032.2	1 034.1	1 032.7	1 031.4	1 009.1	1 027.5	1 034.4	1 032.3	1 029.2	1 030.4
Flow rate [m3/h]	590.00	590.00	590.00	590.00	590.00	590.00	590.00	590.00	590.00	590.00	590.00	590.00	590.00
Flow rate [t/h]	609.77	610.72	609.77	608.97	610.12	609.29	608.51	595.35	606.21	610.28	609.06	607.24	607.94
Cp [kJ/kgK]	2.52	2.52	2.52	2.51	2.52	2.51	2.51	2.41	2.49	2.52	2.51	2.50	2.50
Power [MW]	4.00	4.22	4.26	3.28	3.06	3.60	3.63	2.24	3.50	3.08	3.89	3.95	3.61
Energy [MWh]	2 973.57	2 834.60	3 171.11	2 364.71	2 277.63	2 588.86	2 700.16	805.06	2 523.03	2 294.74	2 801.02	2 939.36	30 273.84

Figure A.2 – Thermal oil heat exchanger energy balance per month - 2023.

	Jan	Fev	Mar	Apr	May	Jun	Jul	Aug	Sep	Out	Nov	Dez	YTD
Hot gas													
Working time [h]	611.00	587.00	665.00	530.00	429.00	599.00	618.00	223.00	540.00	475.00	672.00	368.00	6675.00
Fan speed [%]	97.71	97.33	97.85	98.00	97.54	97.83	97.84	97.55	97.63	97.58	98.82	99.45	97.93
Density [kg/m3]	0.93	0.93	0.94	0.94	0.95	0.95	0.97	0.97	0.95	0.96	0.93	0.94	0.95
Air mass flow [t/h]	167.21	168.05	170.35	171.27	171.24	171.97	175.71	174.90	171.91	172.43	170.57	172.52	171.51
T 1 [ºC]	349.61	321.38	326.59	277.93	245.40	244.06	224.51	227.15	247.91	256.53	310.11	343.59	281.23
T 3 [º C]	107.72	104.32	101.23	99.79	98.08	97.63	89.76	90.39	96.99	95.69	104.46	102.56	99.05
Cp [kJ/(kgK)]	1.03	1.03	1.03	1.02	1.02	1.02	1.02	1.02	1.02	1.02	1.03	1.03	1.02
Power [MW]	11.58	10.41	10.95	8.66	7.15	7.13	6.69	6.76	7.35	7.86	10.00	11.89	8.87
Energy [MWh]	7077.46	6108.30	7283.21	4590.38	3066.47	4273.74	4133.61	1508.34	3969.42	3732.71	6717.92	4374.06	56835.62
Evaporation													
Particle flow [t/h] wb	31.82	31.69	27.79	26.71	24.50	23.71	23.94	15.42	16.12	15.57	14.24	18.31	22.49
Particle [t] wb	19442.80	18600.83	18480.74	14158.01	10509.86	14200.54	14793.99	3439.70	8705.57	7396.89	9571.78	6739.06	146039.79
Moisture in [%]	40.40	33.14	37.71	29.00	25.38	21.36	27.12	25.59	26.67	29.08	33.87	27.52	29.74
Moisture out [%]	1.43	1.33	1.60	1.44	1.82	1.68	1.87	2.08	1.82	1.91	1.77	2.50	1.77
Power [MW]	8.28	6.73	6.70	4.92	3.85	3.11	4.04	2.42	2.67	2.82	3.05	3.06	4.30
Energy [MWh]	5057.94	3949.55	4454.24	2604.97	1652.49	1864.88	2493.87	539.86	1443.86	1341.50	2050.95	1125.65	28579.78
Efficiency [%]	71.5%	64.7%	61.2%	56.7%	53.9%	43.6%	60.3%	35.8%	36.4%	35.9%	30.5%	25.7%	50.3%

Figure A.3 – Recalor energy balance per month - 2023.

	Jan	Fev	Mar	Apr	May	Jun	Jul	Aug	Sep	Out	Nov	Dez	YTD
Hot gas													
Working time [h]	611.00	586.00	639.00	519.00	418.00	600.00	616.00	219.00	541.00	452.00	663.00	378.00	6242.00
Fan speed [%]	63.66	64.39	64.83	65.62	66.89	66.07	67.40	67.57	67.61	68.31	65.79	65.78	66.16
Density [kg/m3]	0.92	0.93	0.93	0.94	0.95	0.95	0.96	0.96	0.94	0.95	0.93	0.94	0.94
Air mass flow [t/h]	126.12	127.57	128.44	130.00	132.52	130.90	133.52	133.86	133.94	135.32	130.34	130.31	131.07
T 1 [ºC]	415.05	383.47	392.07	343.02	308.98	311.38	285.50	294.80	302.02	326.05	385.97	397.22	345.46
T 3 [º C]	107.77	105.36	103.38	100.84	99.58	99.30	92.05	92.04	99.81	98.42	106.51	103.54	100.72
Cp [kJ/(kgK)]	1.04	1.03	1.03	1.03	1.03	1.03	1.02	1.02	1.03	1.03	1.03	1.03	1.03
Power [MW]	11.07	10.14	10.60	9.00	7.93	7.93	7.38	7.76	7.74	8.80	10.41	10.94	9.14
Energy [MWh]	6766.43	5941.09	6770.53	4669.47	3314.88	4759.90	4546.94	1698.50	4186.91	3978.76	6901.01	4133.86	57668.30
Evaporation													
Particle flow [t/h] wb	35.54	28.35	27.26	24.52	23.80	24.12	27.14	21.84	24.23	26.33	24.17	31.64	26.58
Particle [t] wb	21717.05	16610.88	17418.50	12726.70	9949.22	14474.97	16717.02	4782.34	13107.30	11902.64	16022.91	11961.45	167390.97
Moisture in [%]	36.92	32.43	33.62	31.63	29.51	30.83	29.66	31.04	29.82	32.61	35.85	35.21	32.43
Moisture out [%]	1.42	1.37	1.58	1.71	1.78	1.74	1.94	2.19	1.48	1.64	1.08	0.90	1.57
Power [MW]	8.42	5.88	5.83	4.90	4.41	4.68	5.02	4.21	4.58	5.44	5.61	7.25	5.52
Energy [MWh]	5145.30	3443.65	3724.98	2541.12	1841.39	2810.65	3093.56	921.08	2479.25	2459.90	3718.08	2739.42	34918.38
Efficiency [%]	76.0%	58.0%	55.0%	54.4%	55.5%	59.0%	68.0%	54.2%	59.2%	61.8%	53.9%	66.3%	60.6%

Figure A.4 – BSH energy balance per month - 2023.

		Jan	Fev	Mar	Apr	May	Jun	Jul	Aug	Sep	Out	Nov	Dez	YTD
Working time [h]		574.02	583.95	646.37	516.33	419.81	585.44	613.73	219.41	526.21	440.24	620.93	359.76	6 106.20
Circuit 1	T in [ºC]	247.60	247.60	247.60	247.60	247.60	247.60	247.60	247.60	247.60	247.60	247.60	247.60	247.60
	T out [ºC]	230.30	230.30	230.30	230.30	230.30	230.30	230.30	230.30	230.30	230.30	230.30	230.30	230.30
	Flow rate [t/h]	233.56	233.56	233.56	233.56	233.56	233.56	233.56	233.56	233.56	233.56	233.56	233.56	233.56
	Cp [kJ/kgK]	2.47	2.47	2.47	2.47	2.47	2.47	2.47	2.47	2.47	2.47	2.47	2.47	2.47
	Power [MW]	2.77	2.77	2.77	2.77	2.77	2.77	2.77	2.77	2.77	2.77	2.77	2.77	2.77
	Energy [MWh]	1 591.37	1 618.90	1 791.95	1 431.43	1 163.85	1 623.03	1 701.46	608.28	1 458.83	1 220.49	1 721.42	997.37	16 928.37
Circuit 2	T in [ºC]	243.20	243.20	243.20	243.20	243.20	243.20	243.20	243.20	243.20	243.20	243.20	243.20	243.20
	T out [ºC]	237.80	237.80	237.80	237.80	237.80	237.80	237.80	237.80	237.80	237.80	237.80	237.80	237.80
	Flow rate [t/h]	507.05	507.05	507.05	507.05	507.05	507.05	507.05	507.05	507.05	507.05	507.05	507.05	507.05
	Cp [kJ/kgK]	2.47	2.47	2.47	2.47	2.47	2.47	2.47	2.47	2.47	2.47	2.47	2.47	2.47
	Power [MW]	1.88	1.88	1.88	1.88	1.88	1.88	1.88	1.88	1.88	1.88	1.88	1.88	1.88
	Energy [MWh]	1 080.15	1 098.84	1 216.29	971.59	789.97	1 101.64	1 154.87	412.87	990.19	828.41	1 168.42	676.97	11 490.22
Circuit 3	T in [ºC]	239.70	239.70	239.70	239.70	239.70	239.70	239.70	239.70	239.70	239.70	239.70	239.70	239.70
	T out [ºC]	236.90	236.90	236.90	236.90	236.90	236.90	236.90	236.90	236.90	236.90	236.90	236.90	236.90
	Flow rate [t/h]	211.87	211.87	211.87	211.87	211.87	211.87	211.87	211.87	211.87	211.87	211.87	211.87	211.87
	Cp [kJ/kgK]	2.47	2.47	2.47	2.47	2.47	2.47	2.47	2.47	2.47	2.47	2.47	2.47	2.47
	Power [MW]	0.41	0.41	0.41	0.41	0.41	0.41	0.41	0.41	0.41	0.41	0.41	0.41	0.41
	Energy [MWh]	233.48	237.52	262.91	210.02	170.76	238.13	249.64	89.25	214.04	179.07	252.56	146.33	2 483.70
Circuit 4	T in [ºC]	203.30	203.30	203.30	203.30	203.30	203.30	203.30	203.30	203.30	203.30	203.30	203.30	203.30
	T out [ºC]	201.10	201.10	201.10	201.10	201.10	201.10	201.10	201.10	201.10	201.10	201.10	201.10	201.10
	Flow rate [t/h]	143.42	143.42	143.42	143.42	143.42	143.42	143.42	143.42	143.42	143.42	143.42	143.42	143.42
	Cp [kJ/kgK]	2.37	2.37	2.37	2.37	2.37	2.37	2.37	2.37	2.37	2.37	2.37	2.37	2.37
	Power [MW]	0.21	0.21	0.21	0.21	0.21	0.21	0.21	0.21	0.21	0.21	0.21	0.21	0.21
	Energy [MWh]	119.36	121.43	134.41	107.37	87.30	121.74	127.62	45.62	109.42	91.54	129.12	74.81	1 269.72
Circuit 5	T in [ºC]	196.40	196.40	196.40	196.40	196.40	196.40	196.40	196.40	196.40	196.40	196.40	196.40	196.40
	T out [ºC]	195.20	195.20	195.20	195.20	195.20	195.20	195.20	195.20	195.20	195.20	195.20	195.20	195.20
	Flow rate [t/h]	123.77	123.77	123.77	123.77	123.77	123.77	123.77	123.77	123.77	123.77	123.77	123.77	123.77
	Cp [kJ/kgK]	2.36	2.36	2.36	2.36	2.36	2.36	2.36	2.36	2.36	2.36	2.36	2.36	2.36
	Power [MW]	0.10	0.10	0.10	0.10	0.10	0.10	0.10	0.10	0.10	0.10	0.10	0.10	0.10
	Energy [MWh]	55.78	56.74	62.81	50.17	40.79	56.89	59.64	21.32	51.13	42.78	60.34	34.96	593.36
Total power [MW]		5.37	5.37	5.37	5.37	5.37	5.37	5.37	5.37	5.37	5.37	5.37	5.37	5.37
Total energy [MWh]		3 080.15	3 133.43	3 468.37	2 770.59	2 252.67	3 141.42	3 293.23	1 177.34	2 823.60	2 362.29	3 331.86	1 930.44	32 765.38

Figure A.5 – Continuous line press energy balance per month - 2023.

	Jan	Fev	Mar	Apr	May	Jun	Jul	Aug	Sep	Out	Nov	Dez	YTD
BP6													
Working time [h]	229.69	98.41	245.45	174.36	276.16	340.64	246.05	126.99	111.77	76.33	240.13	90.03	2 256.01
Power [MW]	0.26	0.26	0.26	0.26	0.26	0.26	0.26	0.26	0.26	0.26	0.26	0.26	0.26
Energy [MWh]	58.57	25.09	62.59	44.46	70.42	86.86	62.74	32.38	28.50	19.46	61.23	22.96	575.28
BP7													
Working time [h]	355.90	339.97	400.63	293.16	409.66	341.73	405.54	132.06	330.06	363.01	384.97	215.55	3 972.24
Power [MW]	0.64	0.64	0.64	0.64	0.64	0.64	0.64	0.64	0.64	0.64	0.64	0.64	0.64
Energy [MWh]	227.78	217.58	256.40	187.62	262.18	218.71	259.55	84.52	211.24	232.33	246.38	137.95	2 542.23
BP9													
Working time [h]	466.50	482.75	560.00	441.96	288.08	472.89	470.23	92.75	415.70	318.74	389.29	196.79	4 595.68
Power [MW]	0.70	0.70	0.70	0.70	0.70	0.70	0.70	0.70	0.70	0.70	0.70	0.70	0.70
Energy [MWh]	325.52	336.86	390.77	308.40	201.02	329.98	328.13	64.72	290.08	222.42	271.65	137.32	3 206.87

Figure A.6 – BP6, BP7 and BP9 energy balance per month - 2023.

		Jan	Fev	Mar	Apr	May	Jun	Jul	Aug	Sep	Out	Nov	Dez	YTD
Working time [h]		332.12	331.27	385.07	300.13	359.99	356.44	379.05	118.53	310.75	391.84	362.27	176.42	3 803.88
Upper circuit	**T in [ºC]**	184.53	184.11	182.48	183.24	183.53	182.36	183.33	180.55	183.62	182.87	183.73	184.95	183.28
	T out [ºC]	178.40	178.11	176.57	177.41	177.55	176.60	177.55	175.09	177.51	177.06	177.72	178.74	177.36
	Flow rate [t/h]	130.39	130.36	130.23	130.30	130.31	130.23	130.30	130.10	130.31	130.27	130.33	130.42	130.29
	Cp [kJ/kgK]	2.32	2.32	2.31	2.31	2.31	2.31	2.31	2.31	2.31	2.31	2.31	2.32	2.31
	Power [MW]	0.51	0.50	0.49	0.49	0.50	0.48	0.48	0.46	0.51	0.49	0.50	0.52	0.50
	Energy [MWh]	170.66	166.60	190.27	146.29	180.48	171.81	183.44	53.95	159.00	190.48	182.55	91.99	1 887.52
Under circuit	**T in [ºC]**	183.98	183.13	182.63	182.49	182.83	181.66	182.63	181.22	182.73	182.65	183.32	184.12	182.78
	T out [ºC]	179.28	178.61	178.10	178.15	178.57	177.31	178.25	176.84	178.31	178.21	178.79	179.55	178.33
	Flow rate [t/h]	125.90	125.84	125.81	125.80	125.83	125.74	125.81	125.70	125.82	125.81	125.86	125.92	125.82
	Cp [kJ/kgK]	2.32	2.31	2.31	2.31	2.31	2.31	2.31	2.31	2.31	2.31	2.32	2.32	2.31
	Power [MW]	0.38	0.37	0.37	0.35	0.34	0.35	0.35	0.35	0.36	0.36	0.37	0.37	0.36
	Energy [MWh]	126.55	121.10	140.79	105.48	124.18	125.17	134.43	41.87	111.00	140.80	132.98	65.29	1 369.65
Total power [MW]		0.89	0.87	0.86	0.84	0.85	0.83	0.84	0.81	0.87	0.85	0.87	0.89	0.856
Total energy		297.21	287.70	331.06	251.77	304.65	296.98	317.87	95.82	269.99	331.28	315.54	157.28	3 257.16

Figure A.7 – BP8 energy balance per month - 2023.

		Jan	Fev	Mar	Apr	May	Jun	Jul	Aug	Sep	Out	Nov	Dez	YTD
Working time [h]		295.56	297.31	378.36	222.03	323.00	183.02	286.58	53.66	263.14	225.36	175.76	76.78	2 780.56
Circuit 1	T in [ºC]	147.50	147.50	147.50	147.50	147.50	147.50	147.50	147.50	147.50	147.50	147.50	147.50	147.50
	T out [ºC]	142.00	142.00	142.00	142.00	142.00	142.00	142.00	142.00	142.00	142.00	142.00	142.00	142.00
	Flow rate [t/h]	17.22	17.22	17.22	17.22	17.22	17.22	17.22	17.22	17.22	17.22	17.22	17.22	17.22
	Cp [kJ/kgK]	2.22	2.22	2.22	2.22	2.22	2.22	2.22	2.22	2.22	2.22	2.22	2.22	2.22
	Power [MW]	0.06	0.06	0.06	0.06	0.06	0.06	0.06	0.06	0.06	0.06	0.06	0.06	0.06
	Energy [MWh]	17.24	17.34	22.06	12.95	18.84	10.67	16.71	3.13	15.35	13.14	10.25	4.48	162.15
Circuit 2	T in [ºC]	162.50	162.50	162.50	162.50	162.50	162.50	162.50	162.50	162.50	162.50	162.50	162.50	162.50
	T out [ºC]	155.00	155.00	155.00	155.00	155.00	155.00	155.00	155.00	155.00	155.00	155.00	155.00	155.00
	Flow rate [t/h]	17.37	17.37	17.37	17.37	17.37	17.37	17.37	17.37	17.37	17.37	17.37	17.37	17.37
	Cp [kJ/kgK]	2.25	2.25	2.25	2.25	2.25	2.25	2.25	2.25	2.25	2.25	2.25	2.25	2.25
	Power [MW]	0.08	0.08	0.08	0.08	0.08	0.08	0.08	0.08	0.08	0.08	0.08	0.08	0.08
	Energy [MWh]	24.12	24.26	30.88	18.12	26.36	14.94	23.39	4.38	21.47	18.39	14.34	6.27	226.91
Circuit 3	T in [ºC]	159.00	159.00	159.00	159.00	159.00	159.00	159.00	159.00	159.00	159.00	159.00	159.00	159.00
	T out [ºC]	154.00	154.00	154.00	154.00	154.00	154.00	154.00	154.00	154.00	154.00	154.00	154.00	154.00
	Flow rate [t/h]	17.35	17.35	17.35	17.35	17.35	17.35	17.35	17.35	17.35	17.35	17.35	17.35	17.35
	Cp [kJ/kgK]	2.25	2.25	2.25	2.25	2.25	2.25	2.25	2.25	2.25	2.25	2.25	2.25	2.25
	Power [MW]	0.05	0.05	0.05	0.05	0.05	0.05	0.05	0.05	0.05	0.05	0.05	0.05	0.05
	Energy [MWh]	16.01	16.11	20.50	12.03	17.50	9.92	15.53	2.91	14.26	12.21	9.52	4.16	150.65
Circuit 4	T in [ºC]	149.00	149.00	149.00	149.00	149.00	149.00	149.00	149.00	149.00	149.00	149.00	149.00	149.00
	T out [ºC]	141.00	141.00	141.00	141.00	141.00	141.00	141.00	141.00	141.00	141.00	141.00	141.00	141.00
	Flow rate [t/h]	17.23	17.23	17.23	17.23	17.23	17.23	17.23	17.23	17.23	17.23	17.23	17.23	17.23
	Cp [kJ/kgK]	2.22	2.22	2.22	2.22	2.22	2.22	2.22	2.22	2.22	2.22	2.22	2.22	2.22
	Power [MW]	0.08	0.08	0.08	0.08	0.08	0.08	0.08	0.08	0.08	0.08	0.08	0.08	0.08
	Energy [MWh]	25.08	25.23	32.11	18.84	27.41	15.53	24.32	4.55	22.33	19.12	14.92	6.52	235.97
Circuit 5	T in [ºC]	135.00	135.00	135.00	135.00	135.00	135.00	135.00	135.00	135.00	135.00	135.00	135.00	135.00
	T out [ºC]	135.00	135.00	135.00	135.00	135.00	135.00	135.00	135.00	135.00	135.00	135.00	135.00	135.00
	Flow rate [t/h]	17.12	17.12	17.12	17.12	17.12	17.12	17.12	17.12	17.12	17.12	17.12	17.12	17.12
	Cp [kJ/kgK]	2.19	2.19	2.19	2.19	2.19	2.19	2.19	2.19	2.19	2.19	2.19	2.19	2.19
	Power [MW]	-	-	-	-	-	-	-	-	-	-	-	-	-
	Energy [MWh]	-	-	-	-	-	-	-	-	-	-	-	-	-
Total power [MW]		0.28	0.28	0.28	0.28	0.28	0.28	0.28	0.28	0.28	0.28	0.28	0.28	0.28
Total energy [MWh]		82.45	82.94	105.55	61.94	90.11	51.06	79.95	14.97	73.41	62.87	49.03	21.42	775.68

Figure A.8 – VITS1 energy balance per month - 2023.

		Jan	Fev	Mar	Apr	May	Jun	Jul	Aug	Sep	Out	Nov	Dez	YTD
Working time [h]		645.99	624.49	717.26	534.70	612.61	664.09	702.24	97.32	629.13	603.41	655.63	311.50	6 798.37
Circuit 1	T in [ºC]	145	145	145	145	145	145	145	145	145	145	145	145	145.00
	T out [ºC]	144	144	144	144	144	144	144	144	144	144	144	144	144.00
	Flow rate [t/h]	17.22	17.22	17.22	17.22	17.22	17.22	17.22	17.22	17.22	17.22	17.22	17.22	17.22
	Cp [kJ/kgK]	2.22	2.22	2.22	2.22	2.22	2.22	2.22	2.22	2.22	2.22	2.22	2.22	2.22
	Power [MW]	0.01	0.01	0.01	0.01	0.01	0.01	0.01	0.01	0.01	0.01	0.01	0.01	0.01
	Energy [MWh]	6.85	6.62	7.60	5.67	6.49	7.04	7.44	1.03	6.67	6.39	6.95	3.30	72.05
Circuit 2	T in [ºC]	156	156	156	156	156	156	156	156	156	156	156	156	156.00
	T out [ºC]	151	151	151	151	151	151	151	151	151	151	151	151	151.00
	Flow rate [kg/h]	17.32	17.32	17.32	17.32	17.32	17.32	17.32	17.32	17.32	17.32	17.32	17.32	17.32
	Cp [kJ/kgK]	2.24	2.24	2.24	2.24	2.24	2.24	2.24	2.24	2.24	2.24	2.24	2.24	2.24
	Power [MW]	0.05	0.05	0.05	0.05	0.05	0.05	0.05	0.05	0.05	0.05	0.05	0.05	0.05
	Energy [MWh]	34.81	33.65	38.65	28.81	33.01	35.78	37.84	5.24	33.90	32.51	35.33	16.78	366.31
Circuit 3	T in [ºC]	149	149	149	149	149	149	149	149	149	149	149	149	149.00
	T out [ºC]	146	146	146	146	146	146	146	146	146	146	146	146	146.00
	Flow rate [t/h]	17.25	17.25	17.25	17.25	17.25	17.25	17.25	17.25	17.25	17.25	17.25	17.25	17.25
	Cp [kJ/kgK]	2.22	2.22	2.22	2.22	2.22	2.22	2.22	2.22	2.22	2.22	2.22	2.22	2.22
	Power [MW]	0.03	0.03	0.03	0.03	0.03	0.03	0.03	0.03	0.03	0.03	0.03	0.03	0.03
	Energy [MWh]	20.65	19.97	22.93	17.10	19.59	21.23	22.45	3.11	20.11	19.29	20.96	9.96	217.36
Circuit 4	T in [ºC]	155	155	155	155	155	155	155	155	155	155	155	155	155.00
	T out [ºC]	146	146	146	146	146	146	146	146	146	146	146	146	146.00
	Flow rate [t/h]	17.29	17.29	17.29	17.29	17.29	17.29	17.29	17.29	17.29	17.29	17.29	17.29	17.29
	Cp [kJ/kgK]	2.23	2.23	2.23	2.23	2.23	2.23	2.23	2.23	2.23	2.23	2.23	2.23	2.23
	Power [MW]	0.10	0.10	0.10	0.10	0.10	0.10	0.10	0.10	0.10	0.10	0.10	0.10	0.10
	Energy [MWh]	62.31	60.23	69.18	51.57	59.09	64.05	67.73	9.39	60.68	58.20	63.24	30.04	655.71
Circuit 5	T in [ºC]	120	120	120	120	120	120	120	120	120	120	120	120	120.00
	T out [ºC]	115	115	115	115	115	115	115	115	115	115	115	115	115.00
	Flow rate [t/h]	16.93	16.93	16.93	16.93	16.93	16.93	16.93	16.93	16.93	16.93	16.93	16.93	16.93
	Cp [kJ/kgK]	2.14	2.14	2.14	2.14	2.14	2.14	2.14	2.14	2.14	2.14	2.14	2.14	2.14
	Power [MW]	0.05	0.05	0.05	0.05	0.05	0.05	0.05	0.05	0.05	0.05	0.05	0.05	0.05
	Energy [MWh]	32.52	31.43	36.10	26.91	30.84	33.43	35.35	4.90	31.67	30.37	33.00	15.68	342.19
Circuit 6	T in [ºC]	110	110	110	110	110	110	110	110	110	110	110	110	110.00
	T out [ºC]	110	110	110	110	110	110	110	110	110	110	110	110	110.00
	Flow rate [t/h]	16.85	16.85	16.85	16.85	16.85	16.85	16.85	16.85	16.85	16.85	16.85	16.85	16.85
	Cp [kJ/kgK]	2.12	2.12	2.12	2.12	2.12	2.12	2.12	2.12	2.12	2.12	2.12	2.12	2.12
	Power [MW]	-	-	-	-	-	-	-	-	-	-	-	-	-
	Energy [MWh]	-	-	-	-	-	-	-	-	-	-	-	-	-
Total power [MW]		0.24	0.24	0.24	0.24	0.24	0.24	0.24	0.24	0.24	0.24	0.24	0.24	0.24
Total energy [MWh]		157.13	151.90	174.46	130.06	149.01	161.53	170.81	23.67	153.03	146.77	159.47	75.77	1 653.62

Figure A.9 – VITS2 energy balance per month - 2023.

Appendix B

PUMP CURVES

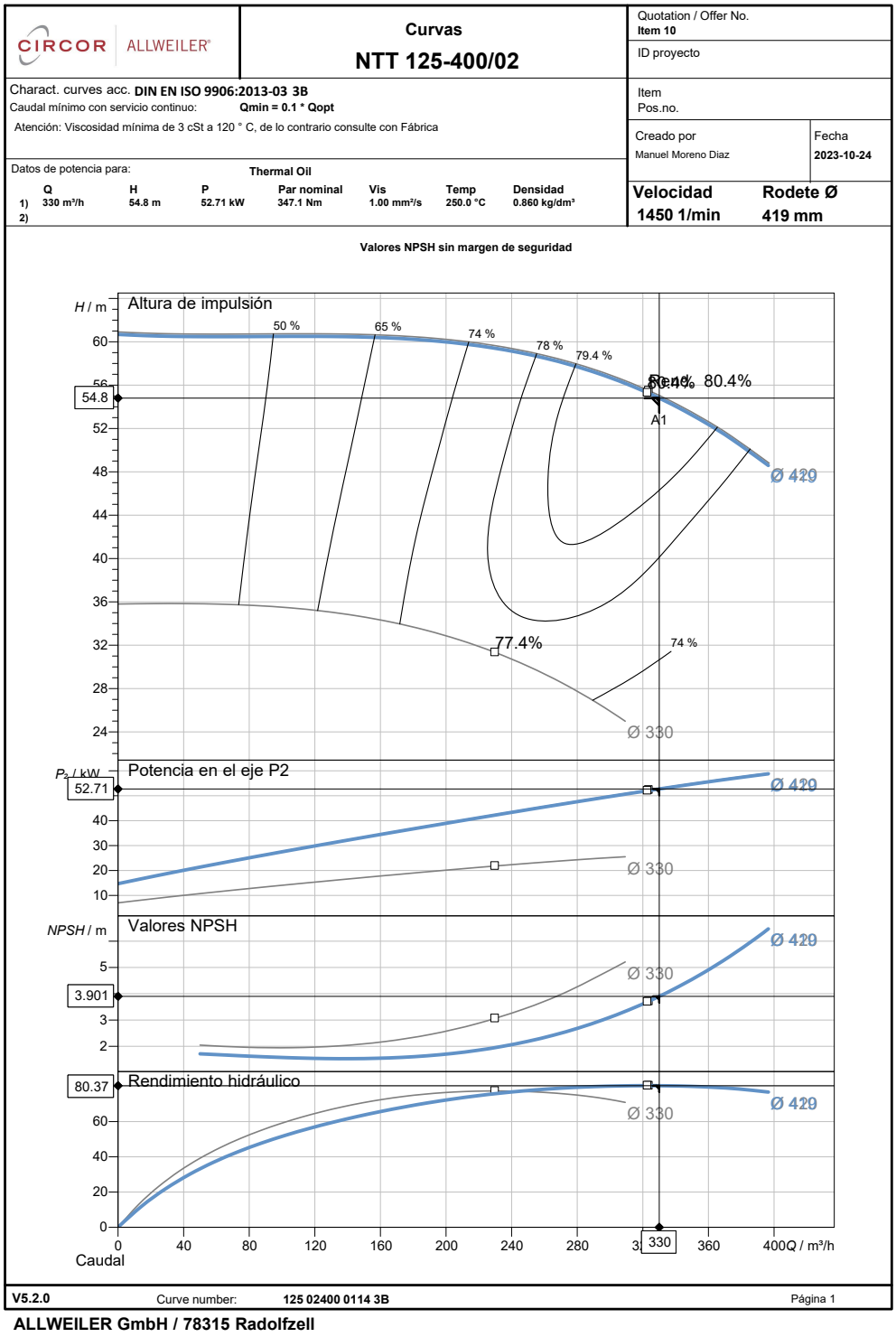

Figure B.1 – Continuous line press circuit 1 pump curves.

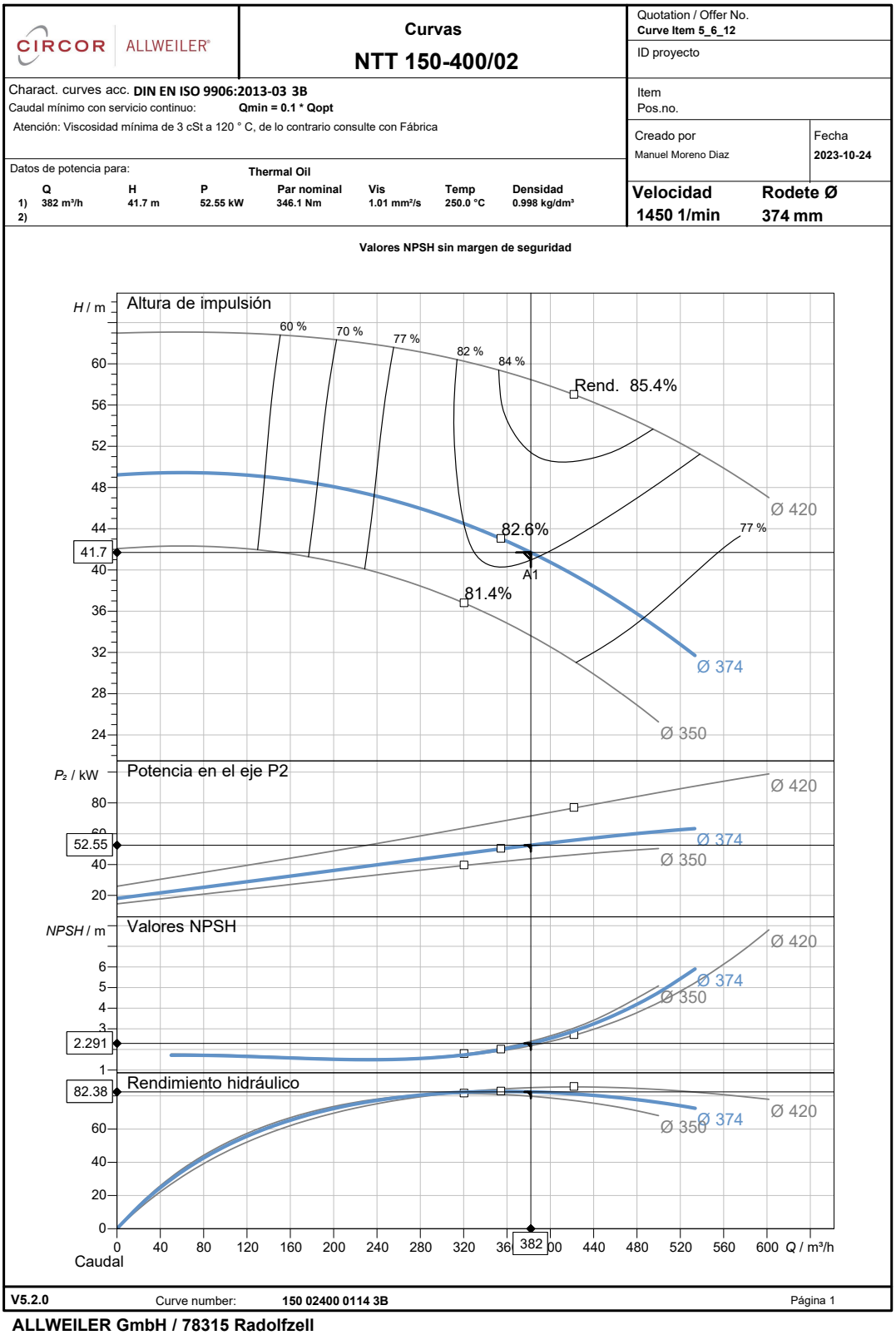

Figure B.2 – Continuous line press circuit 3 pump curves.

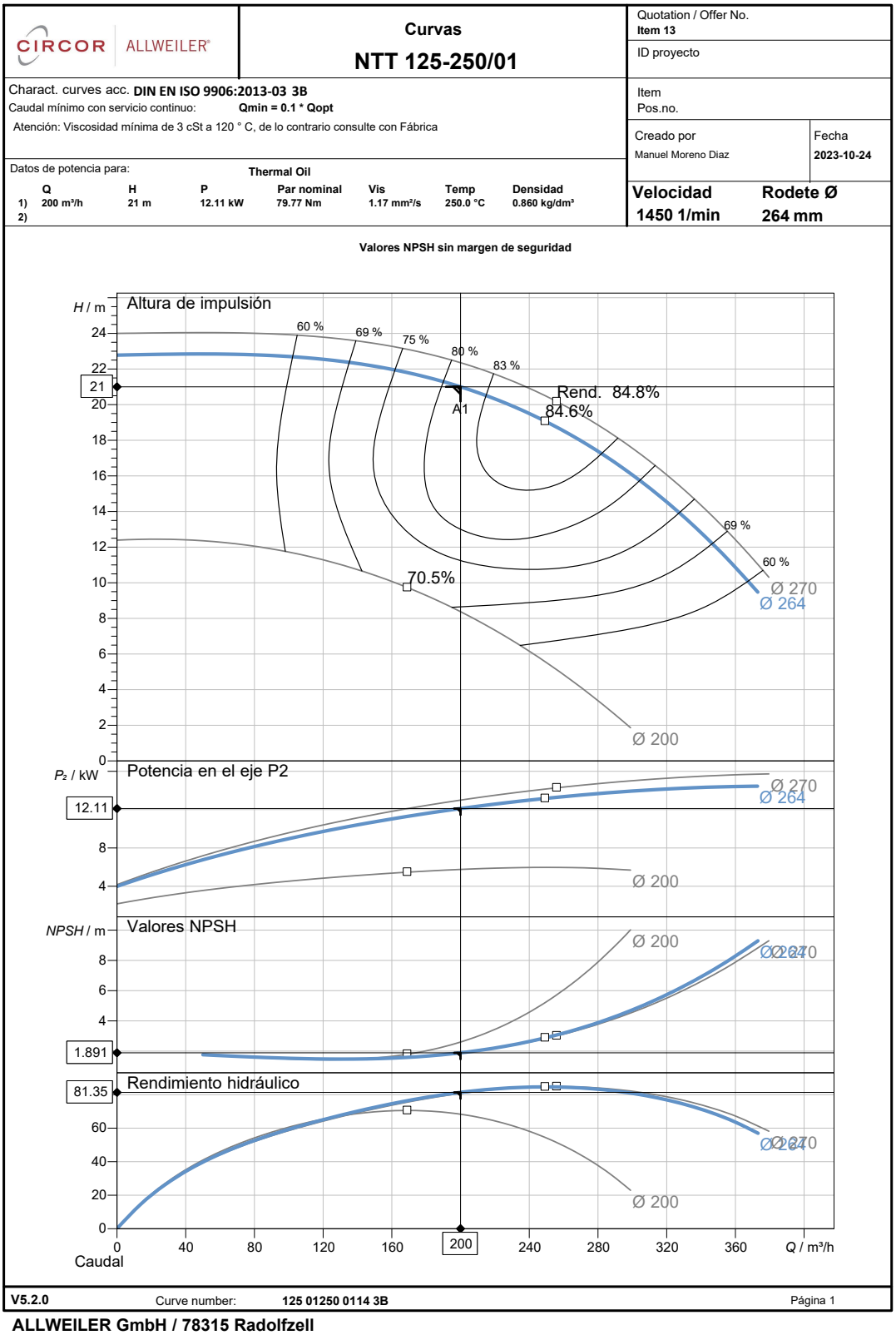

Figure B.3 – Continuous line press circuit 4 and 5 pump curves.

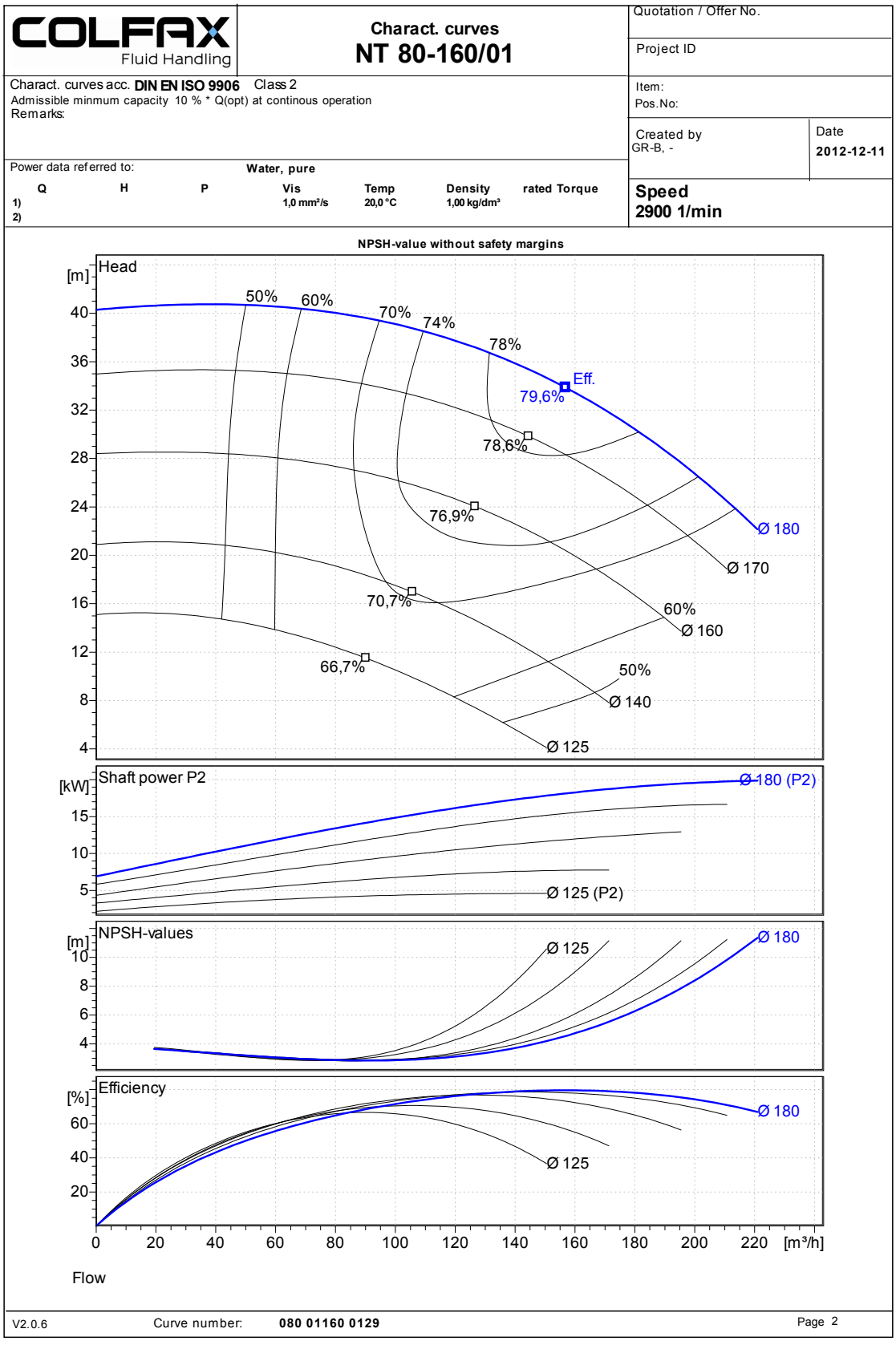

Figure B.4 – Impregnation lines pump curves (ϕ170).